2.3. Immunohistochemical evaluation

A consensus judgment was adopted to establish the proper immunohistochemical scores for tumors, using a scoring system in a previous report [9] that was based on the strength of cytoplasmic expression of CXCR4, CXCR7, CCR6, CCR7, and VEGF: 0, negative; 1+, weak staining; 2+, moderate staining; 3+, strong staining. The distribution of positive cells was also recorded to impart the proportion of positive cells: sporadic (1% ≤ positive cells < 10%); focal (10% ≤ positive cells < 50%); diffuse (positive cells ≥ 50%). The immunohistochemical scores were defined as follows: score 0, no immunoreactivity; score 1, 1+ with sporadic or focal distribution; score 2, 1+ with diffuse distribution or 2+ or 3+ with sporadic distribution; score 3, 2+ with focal or diffuse distribution; score 4, 3+ with focal or diffuse distribution. Then, we considered immunohistochemical scores 0 to 2 as low protein expression and scores 3 and 4 as high protein expression according to our previous study [9].

The degree of angiogenesis was determined by the number of microvessels in defined areas as previously described [9]. The CD31-positive vessels were counted in 4 selected hot spots in a ×400 field (0.26-mm^2 field area). The mean of the 2 independent readings of each specimen was calculated, and microvessel density (MVD) was defined as the mean number of microvessels per 0.26-mm^2 field area.

The MIB-1 labeling index (MIB-1-LI) was estimated by counting the number of positive cells per 1000 tumor cells. Three independent pathologists (Y.O., H.Y., and K.K.), who were not aware of the clinical characteristics of the patients, judged the immunoreactivity. Then, MVD and MIB-1-LI were dichotomized as high or low, based on their median value.

2.4. TaqMan polymerase chain reaction to detect mRNA quantities of CXCR4, CXCR7, CCR6, CCR7, and VEGF

Total RNA was extracted from frozen samples, using Trizol Reagent (Invitrogen, Carlsbad, CA) according to the manufacturer's protocol. Quantitative real-time RT-PCR for these chemokine receptors and for *VEGF* was performed using an ABI PRISM 7700 Sequence Detection System (Applied Biosystems, Foster City, CA) and predeveloped TaqMan assay reagents of human *CXCR4* (spanning exon 1/exon 2; ID: Hs00237052-m1), *CXCR7* (spanning exon 1/exon 2; ID: Hs00604567-m1), *CCR6* (spanning exon 1/exon 2; ID: Hs00171121-m1), *CCR7* (spanning exon 1/exon 2; ID: Hs00171054-m1), *VEGF* (spanning exon 1/exon 2; ID: Hs00173626-m1), and *GAPDH*. The polymerase chain reaction was carried out according to the manufacturer's protocol. The standard curve was constructed with serial dilutions of the *CXCR4*, *CXCR7*, and *VEGF* complementary DNA samples of MCF-7, a breast cancer cell line. As for *CCR6* and *CCR7*, standard curves were constructed using inflamed human tonsils. All reactions of the samples were triplicated, and the data were averaged from the values obtained in each reaction. The obtained data were standardized by using the internal housekeeping gene, *GAPDH*. The final mRNA expression index in each sample was calculated in arbitrary units (AU) as follows: mRNA expression index = *CXCR4*, *CXCR7*, *CCR6*, *CCR7*, or *VEGF* mRNA value/*GAPDH* mRNA value × 1000 AU.

2.5. Statistical analysis

Fisher exact test was used to evaluate the correlation between 2 dichotomous variables. The associations between immunohistochemical scores and mRNA expression were analyzed by the Mann-Whitney *U* test. For univariate and multivariate analyses of overall survival, the Kaplan-Meier method with the log-rank test and Cox proportional hazards model with stepwise procedure were used, respectively. A $P < .05$ was considered statistically significant.

3. Results

3.1. Patient characteristics

Table 1 summarizes the clinical and pathological characteristics of the 78 patients with RMS. The patients consisted of 38 males and 40 females, ranging in age from a month to 71 years old. Histologically, the 82 specimens

Table 1 Clinicopathological characteristics of 78 patients with primary RMS

Parameters	No. of cases (n = 78)
Age (y)	
≤15	53
>15	25
Sex	
Male	38
Female	40
Histology (primary)	
Embryonal	44
Alveolar	34
Stage (at diagnosis)	
1	22
2	5
3	41
4	5
Unknown	5
Location of primary tumor	
Favorable	24
Unfavorable	54
Tumor size (cm)	
≤5	27
>5	45
Unknown	6

Table 2 Results of immunostaining

	CXCR4 (n = 78)	CXCR7 (n = 77)	VEGF (n = 78)	CCR6 (n = 78)	CCR7 (n = 75)
ERMS					
High expression	18 (40.9%)	35 (79.5%)	22 (50.0%)	15 (34.1%)	30 (71.4%)
Low expression	26 (59.1%)	9 (20.5%)	22 (50.0%)	29 (65.9%)	12 (28.6%)
ARMS					
High expression	20 (58.8%)	29 (87.9%)	24 (70.6%)	25 (73.5%)	16 (48.5%)
Low expression	14 (41.2%)	4 (12.1%)	10 (29.4%)	9 (26.5%)	17 (51.5%)
P	.1703	.3760	.1036	.0007 *	.0967

Abbreviations: ERMS, embryonal rhabdomyosarcoma; ARMS, alveolar rhabdomyosarcoma.
* $P < .05$.

included 34 primary ARMS, 44 primary ERMS, 3 metastatic ARMS, and 1 ARMS recurrence. *PAX3/PAX7-FKHR* fusion gene transcripts were examined in 21 cases of 34 ARMS and 15 cases of 44 ERMS. *PAX3-FKHR* fusion gene transcript was identified in 14 ARMS cases, and *PAX7-FKHR* fusion gene transcript was identified in 3 ARMS cases by RT-PCR and direct sequencing. None of *PAX3/PAX7-FKHR* fusion gene transcript was detected in ERMS. Survival data were available in 76 cases, with follow-up periods ranging from 1 to 223 months (median, 17 months). Of the 78 patients, 59 received combined modality therapy including chemotherapy using some of the standardized antitumor drugs (vincristine, actinomycin D, and cyclophosphamide), and 12 patients received surgical treatment and/or radiation therapy, whereas 7 patients had no therapeutic information.

3.2. Immunohistochemistry

Table 2 summarizes the results of immunostaining for CXCR4, CXCR7, VEGF, CCR6, and CCR7. *P* value

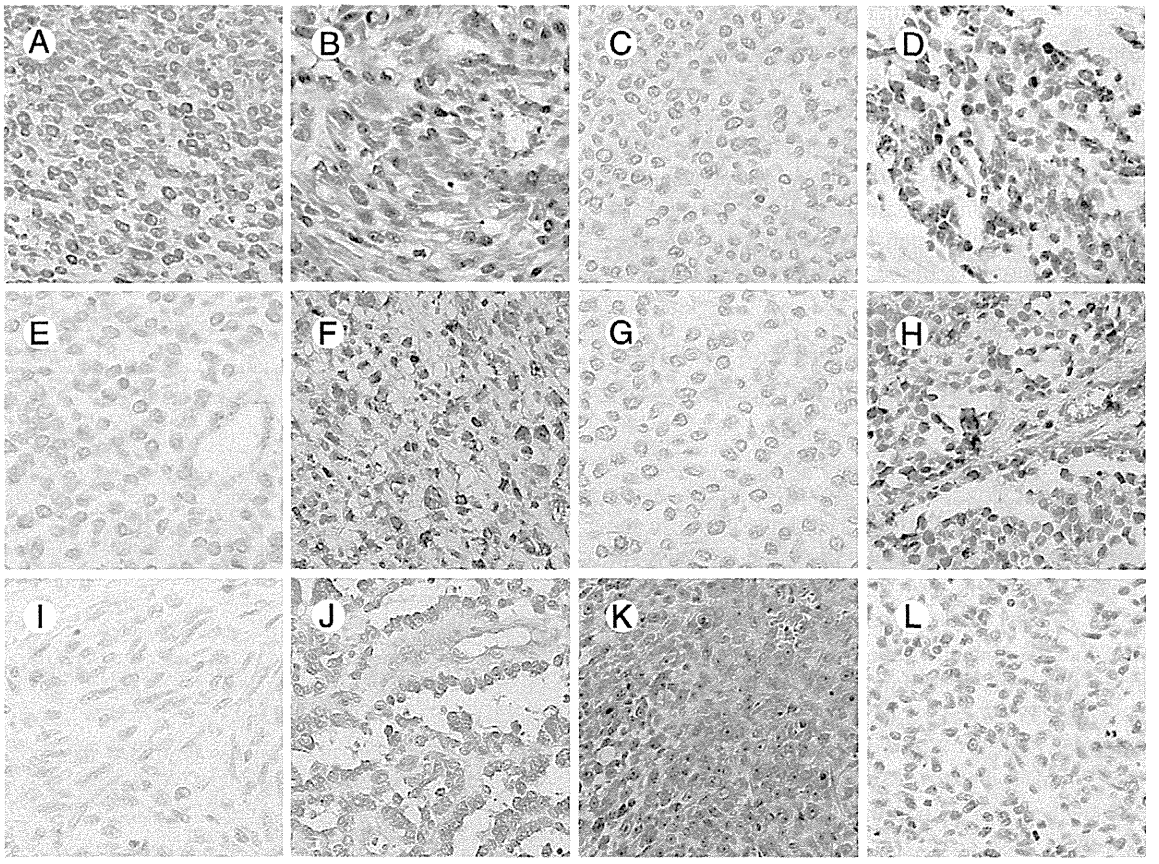

Fig. 1 Results of immunohistochemical expression of CXCR4 (A-C), CXCR7 (D, E), CCR6 (F, G), CCR7 (H, I), and VEGF (J-L) in primary site of RMS. A and B, ARMS (A) and ERMS (B) showing diffuse and strong immunoreactivity for CXCR4, evaluated as score 4. C, Negative staining of CXCR4. D, Diffuse and strong staining of CXCR7 in ARMS. E, Negative staining of CXCR7. F, Focal and strong cytoplasmic expression of CCR6 in ERMS. G, Negative staining of CCR6. H, Alveolar patterned tumor cells revealed diffuse and moderate CCR7 cytoplasmic immunostaining. I, Negative staining of CCR7. J and K, Cytoplasmic diffuse and strong (J) and diffuse and moderate (K) immunoreactivity for VEGF in ARMS (J) and ERMS (K). L, Negative staining of VEGF. Original magnification ×200.

represents the stastical association of the expression of each immunostaining factor between ERMS and ARMS. Positive staining for CXCR7, VEGF, and CCR6 was recognized mainly in the cytoplasm of the tumor cells or endothelium [26], whereas CXCR4 and CCR7 expression was seen in the nucleus as well as the cytoplasm shown in Fig. 1 [9,26].

3.3. CXCR4, CXCR7, and VEGF immunostaining

Of the 78 primary RMS, 38 (48.7%) showed high expression of cytoplasmic CXCR4. High CXCR4 expression was recognized in 20 (58.8%) of 34 in ARMS and 18 (40.9%) of 44 in ERMS. In the same manner, high VEGF expression was observed in 46 (58.9%) of 78 in all the RMS, 24 (70.6%) of 34 in ARMS, and 22 (50%) of 44 in ERMS. High CXCR7 expression was recognized in 64 (83.1%) of 77 in RMS, 29 (87.9%) of 33 in ARMS, and 35 (79.5%) of 44 in ERMS. RMS displayed high CXCR7 expression regardless of the histologic subtype (Table 2). None of these proteins showed expression patterns that differed significantly between the histologic subtypes.

Within the cases that showed high cytoplasmic CXCR4 expression, 19 (55.9%) of 34 ARMS and 14 (31.8%) of 44 ERMS showed high VEGF expression. This revealed a significant association between CXCR4 and VEGF expression (P = .0003 and P = .0051, respectively) as shown in Fig. 2. Immunohistochemical expression of CXCR7 showed no significant association with CXCR4 or VEGF expression in either ARMS or ERMS (CXCR7 versus CXCR4: ARMS P > .9999, ERMS P = .7161; CXCR7 versus VEGF: ARMS P = .2952, ERMS P > .9999; data not shown).

3.4. CCR6 and CCR7 immunostaining

Of 44 cases, 15 (34.1%) showed high CCR6 expression in ERMS, whereas 25 (73.5%) of 34 cases showed high expression in ARMS. High expression of CCR7 was recognized in 30 (71.4%) of 42 in ERMS and 16 (48.5%)

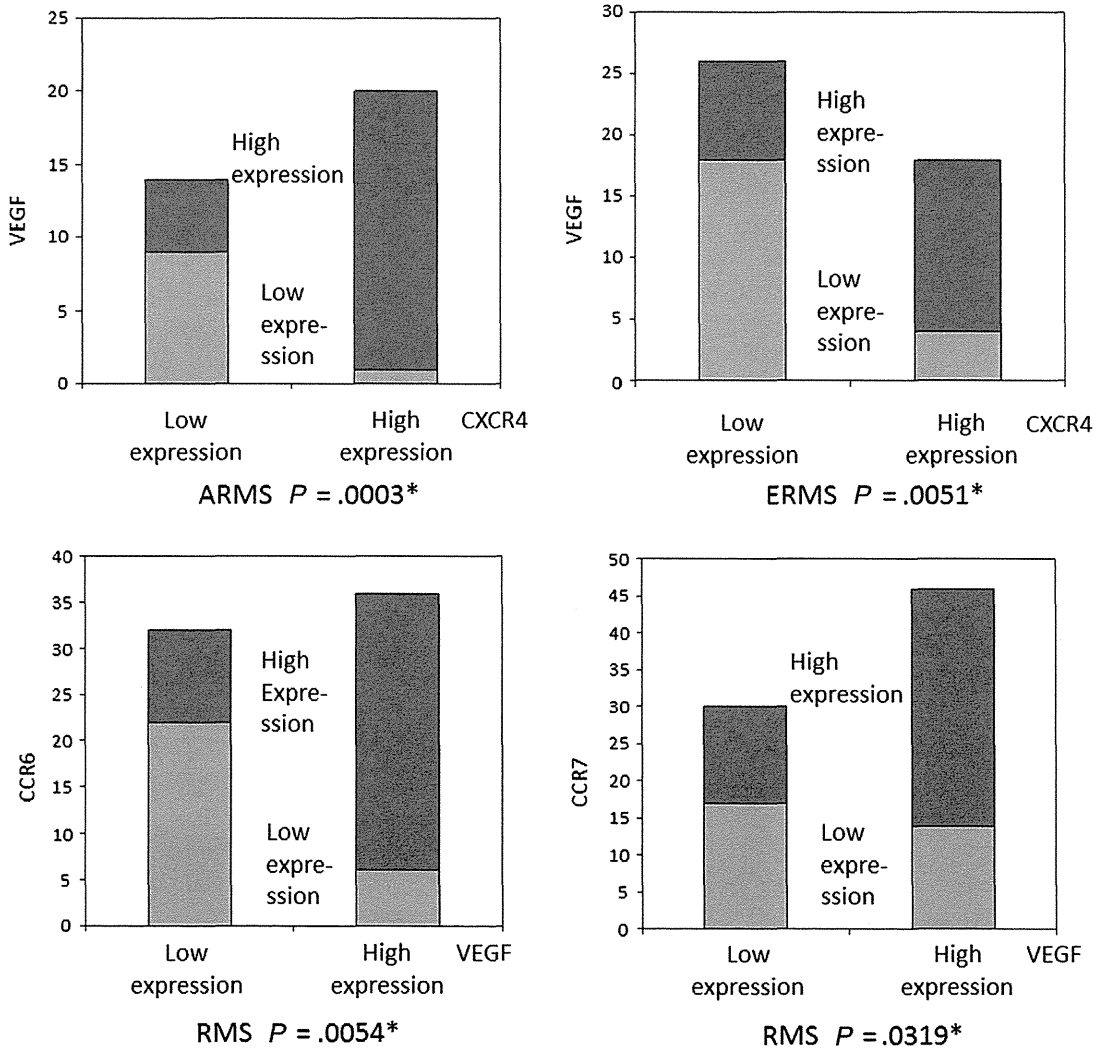

Fig. 2 Association between immunohistochemical score of CXCR4 and VEGF. There were significant positive associations in both ARMS and ERMS. There also are significant associations between VEGF and CCR6 as well as between VEGF and CCR7 in all RMS cases.

Table 3 Microvessel density and MIB-1-LI in RMS

		RMS (n = 78)	ERMS (n = 44)	ARMS (n = 34)	*P*
MVD	Mean ± SD	11.00 ± 6.61	11.13 ± 6.71	10.50 ± 6.46	.996
MIB-1-LI	Mean ± SD	14.15 ± 11.29	12.79 ± 11.85	11.85 ± 8.41	.2189

Abbreviations: MVD, microvessel density; MIB-1-LI, MIB-1 labeling index; RMS, rhabdomyosarcoma; ERMS, embryonal rhabdomyosarcoma; ARMS, alveolar rhabdomyosarcoma.

of 33 in ARMS (Table 2). ARMS cases revealed higher CCR6 expression than ERMS cases, with statistical significance ($P = .0007$), whereas CCR7 expression showed no significant difference between the 2 histologic types ($P = .0967$). CCR6 and CCR7 expression levels showed no association in RMS ($P = .6395$, data not shown). Neither CCR6 nor CCR7 showed an association with either CXCR4 or CXCR7 expression, whereas VEGF expression showed significant associations to both CCR6 expression and CCR7 expression ($P = .0054$ and $P = .0319$, respectively) in all RMS (Fig. 2).

3.5. Microvessel density

MVD was assessed by immunohistochemical staining of CD31. It ranged from 5.5 to 37.25 (median, 11.00 ± 6.61). Median of MVD did not show statistical difference between histologic subtypes (ERMS median, 11.13 ± 6.71; ARMS median, 10.50 ± 6.46; $P = .996$; Table 3). No significant relationship was observed between MVD and immunohistochemical expression of CXCR4, CXCR7, VEGF, CCR6, or CCR7 ($P = .7114$, $P = .1870$, $P = .3071$, $P = .8337$, and $P = .8733$, respectively; data not shown).

3.6. MIB-1 labeling index

The MIB-1-LI ranged from 2.2 to 65.38 (median, 14.15 ± 11.29), and its median of both subtypes showed no statistical difference (ERMS median, 12.79 ± 11.85; ARMS median, 11.85 ± 8.41; $P = .2189$; Table 3). No significant relationship was observed between MIB-1-LI and immunohistochemical expression of CXCR4, CXCR7, VEGF, CCR6, or CCR7 ($P = .0760$, $P = .9458$, $P = .7761$, $P = .4564$, and $P = .8985$, respectively; data not shown).

3.7. Quantitative mRNA expression of CXCR4, CXCR7, VEGF, CCR6, and CCR7 and their immunohistochemical expression

In comparison with the results of immunohistochemistry and quantitative real-time RT-PCR, a statistical association was found between immunohistochemical scores and mRNA expression levels in *CXCR4* and *VEGF* ($P = .0041$ and $P = .0235$, respectively; Fig. 3), whereas *CXCR7*, *CCR6*, and *CCR7* revealed no association ($P = .2706$, $P = .5067$, and $P = .1998$, respectively).

3.8. Survival analysis

Tables 4 and 5 summarize the results of survival analysis in all RMS cases and RMS groups separated by subtypes. By univariate analysis of ERMS cases, a poorer likelihood of survival has been revealed in the groups with high VEGF expression compared with the groups with low expression (Fig. 4, $P = .0017$). Especially about receptors expression, VEGF expression and CCR6 expression appeared to be an independent prognostic factor for ERMS ($P = .0008$ and $P = .042$, respectively; Table 5).

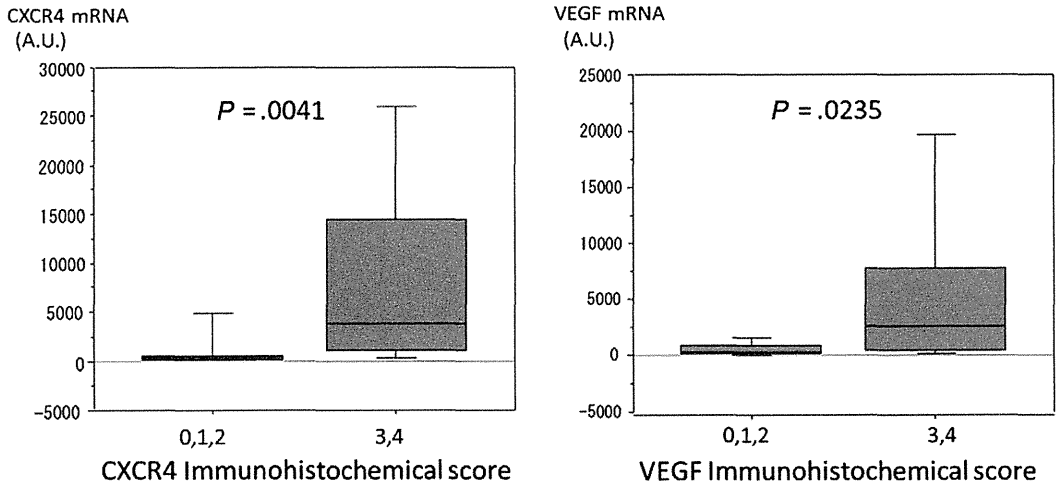

Fig. 3 Association between immunohistochemical expression status of CXCR4 and VEGF and their mRNA protein expression. The immunohistochemical status was associated with the corresponding mRNA expression.

Table 4 Univariate analysis for overall survival

Variables	RMS		ERMS		ARMS	
	No. of cases	*P*		*P*		*P*
Age		.0071 *		.0375 *		.0246 *
<15	50		33		17	
≥15	22		5		17	
Sex		.7076		.6263		.6863
Male	34		17		17	
Female	38		21		17	
Histology		.0306 *				
ERMS	38					
ARMS	34					
Tumor size		.0611		.0456 *		.4301
≤5 cm	25		12		13	
5 cm	41		24		17	
Location		.0255 *		.4496		.2066
Favorable	22		13		9	
Unfavorable	50		25		25	
Stage		.0102 *		.1946		.2791
1,2	25		16		9	
3,4	42		20		22	
CXCR4		.2560		.3477		.7397
High	35		15		20	
Low	37		23		14	
CXCR7		.0414 *		.0869		.1801
High	59		30		29	
Low	12		8		4	
VEGF		.0001 *		.0010 *		.1336
High	45		21		24	
Low	27		17		10	
CCR6		.3098		.9695		.4599
High	39		14		25	
Low	33		24		9	
CCR7		.6119		.3428		.6429
High	41		25		16	
Low	30		12		17	
MVD		.2707		.1892		.1933
≤11	36		19		17	
>11	36		19		17	
MIB-1-LI		.0480 *		.0262 *		.0258 *
≤14.15	36		14		22	
>14.15	36		24		12	

Abbreviations: MVD, microvessel density; MIB-1-LI, MIB-1 labeling index; RMS, rhabdomyosarcoma; ERMS, embryonal rhabdomyosarcoma; ARMS, alveolar rhabdomyosarcoma.

* $P < .05$.

Only the VEGF expression came up as independent prognostic factors in ARMS ($P = .0353$; Table 5).

MVD did not affect survival in all RMS, whereas low MIB-1-LI in all RMS correlated significantly with poor survival in univariate analysis ($P = .048$; Table 4).

4. Discussion

CXCR4, a receptor for its sole ligand, SDF-1 (SDF-1/CXCL12), is known to be related to chemotaxis and homing, which are important steps in tumor metastasis [3,4]. Previous retrospective studies show that CXCR4 is highly expressed in various cancers and that its overexpression is closely correlated with lung, liver, and bone marrow metastasis as well as poor prognosis in several kinds of malignant solid tumors [4-7,9].

The important role of the CXCR4/SDF-1 pathway in tumor spread and metastasis has been demonstrated in RMS cell lines [6,7]. Especially, the cell lines derived from ARMS expressed higher levels of CXCR4 than cell lines derived from ERMS. A recent study found a significant correlation between high immunohistochemical expression of CXCR4 and poor prognosis in a clinical series of 40 RMS cases [27]. Those authors also noted significantly higher levels of CXCR4 expression in alveolar histology.

In the present study, there was no significant difference in the immunohistochemical expression of CXCR4 between the 2 histologic subtypes. However, almost half of RMS showed high CXCR4 expression. It is demonstrated that CXCR4 antagonists inhibit the primary tumor and metastasis in animal models of melanoma and osteosarcoma [5]. Therefore, CXCR4 could be a candidate for molecular target therapy in RMS with high CXCR4 expression.

We have also revealed significantly higher CCR6 expression in ARMS, and the present study is the first to investigate the CCR6 immunohistochemical expression status with RMS histology.

Recently, CXCR7 was identified as a receptor for SDF-1, and the SDF-1/CXCR7 axis was reported to regulate the metastatic potential of human RMS cells, similarly to SDF-1/CXCR4 [10]. Among RMS cells, ERMS cells express CXCR7 highly and express very low levels of CXCR4, whereas ARMS-like cells express CXCR4 highly and down-regulate CXCR7 expression [28]. In our study, no significant difference in the expression rate of CXCR7 was revealed, although CXCR7 showed consistently high expression in both histologic subtypes (ARMS: 87.9%, ERMS: 79.5%). It is reported that, in a hepatocellular carcinoma cell line, down-regulation of CXCR7 inhibits the growth and invasion of tumor cells, which indicates that CXCR7 may be a potential target for molecular targeted therapy [29]. Possibility for application of the CXCR7 antagonists to RMS, which widely expresses CXCR7, could be worth pursuing in the future.

Overexpression of VEGF has been reported in various epithelial malignancies and is thought to be a potent regulator of angiogenesis. Gee et al [30] have shown that the VEGF and VEGF family receptor mRNAs were expressed in RMS cell lines. However, we could not find any investigations into VEGF expression in large series of clinical RMS specimens. We demonstrated significantly more frequent VEGF expression in ARMS than in ERMS. Considering the statistical difference in prognosis between the subtypes, VEGF could still be a potential therapeutic target in ARMS, which is destined for poorer prognosis,

Bachelder et al [8] demonstrated that VEGF regulates CXCR4 expression in breast carcinoma cells. They also demonstrated that CXCR4 mediates the migration of breast

Table 5 Multivariate analysis in RMS

	RMS (n = 70)		ERMS (n = 40)		ARMS (n = 30)	
Variables	*P*	HR (95% CI)	*P*	HR (95% CI)	*P*	HR (95% CI)
Age	.0002 *	0.221 (0.099-0.492)	.0019 *	0.068 (0.012-0.369)	.0201 *	0.345 (0.14-0.847)
Tumor size (≤5 cm *vs* >5 cm)	.0708	0.515 (0.251-1.058)	.0527 *	0.312 (0.096-1.014)		
Location (favorable *vs* unfavorable)					.1005	0.387 (0.125-1.201)
CXCR4 (high *vs* low)	.0145 *	2.824 (1.228-6.491)			.0716	3.287 (0.901-11.995)
CXCR7 (high *vs* low)						
VEGF (high *vs* low)	<.0001 *	0.113 (0.04-0.313)	.0008 *	0.124 (0.036-0.422)	.0353 *	0.21 (0.049-0.898)
CCR6 (high *vs* low)	.0181 *	2.403 (1.162-4.970)	.042 *	3.778 (1.049-13.609)		
CCR7 (high *vs* low)						

Abbreviations: HR, hazard ratio; CI, confidence interval; RMS, rhabdomyosarcoma; ERMS, embryonal rhabdomyosarcoma; ARMS, alveolar rhabdomyosarcoma.

* $P < .05$.

cancer cells, depending on autocrine VEGF. Since then, a close correlation between CXCR4 and VEGF expression has been demonstrated in several types of malignancies [21] and in osteosarcoma [31] in vitro and in vivo. In our previous study, we have investigated the CXCR4 and VEGF expression in soft tissue sarcoma. Nine primary RMS were included in the category of malignant round cell tumors and revealed higher mRNA levels of *CXCR4* and *VEGF* than the control skeletal muscle tissue. However, we could not detect significant association between mRNA expression levels for *CXCR4* and *VEGF* in a small number of malignant round cell tumor. In the present study, we confirmed the significant positive correlation between immunohistochemical CXCR4 and VEGF expression. To our knowledge, no other report refers to the correlation between VEGF and CXCR4 in a large series of clinical RMS.

The correlation between MVD and VEGF expression level and prognosis has been controversial, as some reports have failed to reveal a correlation in several solid tumors [17] or in soft tissue sarcomas [32], whereas other reports have questioned it in soft tissue sarcomas [33,34]. In the present study, we could not find correlation between MVD and VEGF or any other immunohistochemical factors in RMS. Moreover, MVD did not correlate with outcome. A similar result was reported in a study with soft tissue sarcomas that compared MVD and tissue VEGF concentration [33].

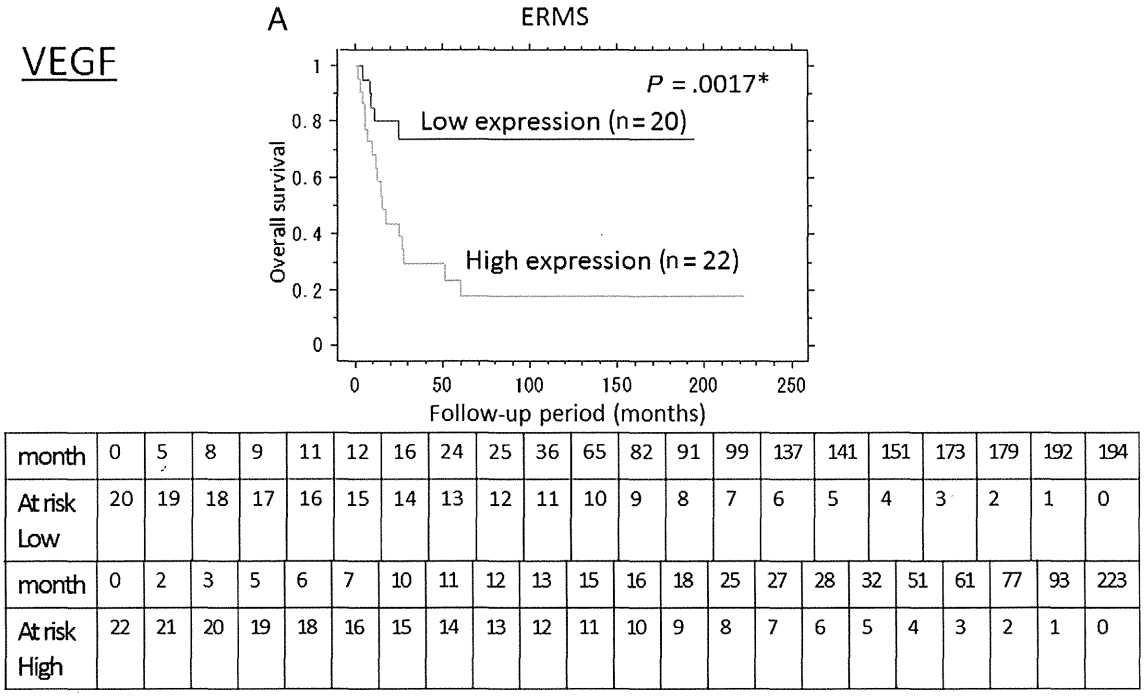

month	0	5	8	9	11	12	16	24	25	36	65	82	91	99	137	141	151	173	179	192	194
At risk Low	20	19	18	17	16	15	14	13	12	11	10	9	8	7	6	5	4	3	2	1	0
month	0	2	3	5	6	7	10	11	12	13	15	16	18	25	27	28	32	51	61	77	93	223
At risk High	22	21	20	19	18	16	15	14	13	12	11	10	9	8	7	6	5	4	3	2	1	0

Fig. 4 Difference in overall survival between histologic subtypes of RMS. A high VEGF expression in ERMS (A) showed significantly poorer prognosis, but not in ARMS (B).

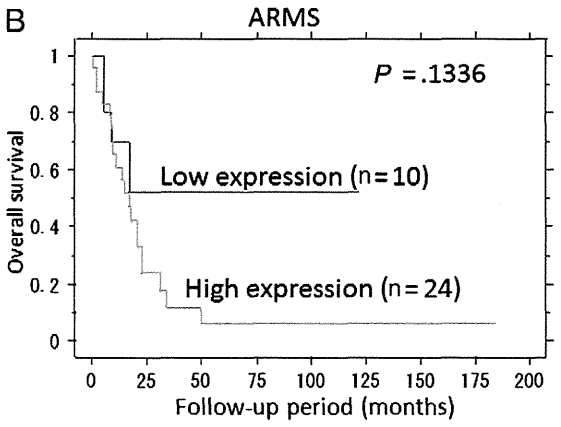

Month	0	6	9	10	11	14	17	28	102	122
At risk	10	9	7	6	5	4	3	2	1	0

month	0	1	2	5	8	9	10	11	14	15	17	18	21	23	28	31	34	50	184
At risk High	24	23	21	20	18	17	14	13	12	11	10	9	7	5	4	3	2	1	0

Fig. 4 *(continued).*

Other chemokine receptors, CCR6 and CCR7, have been revealed to bind to CCL20 and CCL 19/21 with involvement in liver metastases and lymph node metastases in gastrointestinal carcinoma [12,13]. CCL20 was originally identified in the liver and was the only chemokine known to interact with CCR6. Thus, the receptor-ligand pair CCR6-CCL20 plays an important role in the chemoattraction of T cells to the liver [35]. In our series of RMS, none of the patients developed liver metastasis, but ARMS showed frequently higher CCR6 expression than ERMS. The importance of chemokine receptors in metastasis is mostly related to CXCR4 and CCR7, aside from the correlation between CXCR4 and organ-specific metastases such as those of lung, liver, and bone marrow, CCR7 expression generally correlates with increased lymph node metastases [11,12]. In our study, high CCR7 expression showed no relation with other immunohistochemical factors.

In conclusion, both ARMS and ERMS displayed association between VEGF and CXCR4 expression. In addition, our results suggest that high VEGF expression may be predictive prognostic factors in RMS. Considering that RMS widely expresses CXCR4 and CXCR7, these chemokine receptors and VEGF may provide potential targets of molecular therapy as part of combined modality therapy in RMS.

Acknowledgment

The English usage in this article was reviewed by KN International (http://www.kninter.com/).

References

[1] Parham DM, Barr FG. Embryonal rhabdomyosarcoma and alveolar rhabdomyosarcoma. In: Fletcher CDM, Bridge JA, Hogendoorn PCW, Mertens F, editors. World Health Organization Classification of Tumours, Pathology and Genetics of Tumours of Soft Tissue and Bone. 4th ed. Lyon: IARC Press; 2013. p. 127-35.

[2] Zlotnik A, Burkhardt AM, Homey B. Homeostatic chemokine receptors and organ-specific metastasis. Nat Rev Immunol 2011;11:597-606.

[3] Muller A, Homey B, Soto H, et al. Involvement of chemokine receptors in breast cancer metastasis. Nature 2001;410:50-6.

[4] Taichman RS, Cooper C, Keller ET, et al. Use of the stromal cell-derived factor-1/CXCR4 pathway in prostate cancer metastasis to bone. Cancer Res 2002;62:1832-7.

[5] Kim SY, Lee CH, Midura BV, et al. Inhibition of the CXCR4/CXCL12 chemokine pathway reduces the development of murine pulmonary metastases. Clin Exp Metastasis 2008;25:201-11.

[6] Libura J, Drukala J, Majka M, et al. CXCR4-SDF-1 signaling is active in rhabdomyosarcoma cells and regulates locomotion, chemotaxis, and adhesion. Blood 2002;100:2597-606.

[7] Strahm B, Durbin AD, Sexsmith E, et al. The CXCR4-SDF1 axia is a critical mediator of rhabdomyosarcoma metastatic signaling induced by bone marrow stroma. Clin Exp Metastasis 2008;25:1-10.

[8] Bachelder RE, Wendt MA, Mercurio AM. Vascular endothelial growth factor promotes breast carcinoma invasion in an autocrine manner by regulating the chemokine receptor CXCR4. Cancer Res 2002;62:7203-6.

[9] Oda Y, Yamamoto H, Tamiya S, et al. CXCR4 and VEGF expression in the primary site and the metastatic site of human osteosarcoma: analysis within a group of patients, all of whom developed lung metastasis. Mod Pathol 2006;19:738-45.

[10] Balkwill F. The significance of cancer cell expression of CXCR4. Semin Cancer Biol 2004;14:171-9.

[11] Takanami I. Overexpression of CCR7 mRNA in nonsmall cell lung cancer: correlation with lymph node metastasis. Int J Cancer 2003;105:186-9.

[12] Günther K, Leier J, Henning G, et al. Prediction of lymph node metastasis in colorectal carcinoma by expression of chemokine receptor CCR7. Int J Cancer 2005;116:726-33.
[13] Ghadjar P, Coupland SE, Na IK, et al. Chemokine receptor CCR6 expression level and liver metastases in colorectal cancer. J Clin Oncol 2006;24:1910-6.
[14] Ghadjar P, Loddenkemper C, Coupland SE, et al. Chemokine receptor CCR6 expression level and aggressiveness of prostate cancer. J Cancer Res Clin Oncol 2008;134:1181-9.
[15] Dvorak HF. Vascular permeability factor/vascular endothelial growth factor: A critical cytokine in tumor angiogenesis and a potential target for diagnosis and therapy. J Clin Oncol 2002;20:4368-80.
[16] Ferrara N, Hillan HP, Gerber W, et al. Discovery and development of bevacizumab, an anti-VEGF antibody for treating cancer. Nat Rev Drug Discov 2004;3:391-400.
[17] Ferrara N. VEGF as a therapeutic target in cancer. Oncology 2005;69:11-6.
[18] Semenza GL. A new weapon for attacking tumor blood vessels. N Engl J Med 2008;358:2066-7.
[19] Burns JM, Summers BC, Wang Y, et al. A novel chemokine receptor for SDF-1 and I-TAC involved in cell survival, cell adhesion, and tumor development. J Exp Med 2006;203:2201-13.
[20] Grymula K, Tarnowski M, Wysoczynski M, et al. Overlapping and distinct role of CXCR7-SDF-1/ITAC and CXCR4-SDF-1 axes in regulating metastatic behavior of human rhabdomyosarcomas. Int J Cancer 2010;127:2554-68.
[21] Liang Z, Brooks J, Willard M, et al. CXCR4/CXCL12 axis promotes VEGF-mediated tumor angiogenesis through Akt signaling pathway. Biochem Biophys Res Commun 2007;359:716-22.
[22] Billadeau DD, Chatterjee S, Bramati P, et al. Characterization of CXCR4 signaling in pancreatic cancer cells. Int J Gastrointest Cancer 2006;37:110-9.
[23] Lawrence Jr W, Anderson JR, Gehan EA, et al. Pretreatment TNM staging of childhood rhabdomyosarcoma: a report of the Intergroup Rhabdomyosarcoma Study Group. Children's Cancer Study Group. Pediatric Oncology Group. Cancer 1997;80:1165-70.
[24] Oda Y, Tateishi N, Matono H, et al. Chemokine receptor CXCR4 expression is correlated with VEGF expression and poor survival in soft-tissue sarcoma. Int J Cancer 2009;124:1852-9.
[25] Wang L, Chen W, Gao L, et al. High expression of CXCR4, CXCR7 and SDF-1 predicts poor survival in renal cell carcinoma. World J Surg Oncol 2012;10:212.
[26] Toyozawa S, Yamamoto Y, Ishida Y, et al. Immunohistochemical analysis of CXCR4 expression in fibrohistiocytic tumors. Acta Histochem Cytochem 2010;43:45-50.
[27] Diomedi-Camassei F, McDowell HP, De Ioris MA, et al. Clinical significance of CXC chemokine receptor-4 and c-Met in childhood rhabdomyosarcoma. Clin Cancer Res 2008;14:4119-27.
[28] Tarnowski M, Grymula K, Reca R, et al. Regulation of expression of stromal-derived factor-1 receptors: CXCR4 and CXCR7 in human rhabdomyosarcomas. Mol Cancer Res 2010;8:1-14.
[29] Xue TC, Chen RX, Han D, et al. Down-regulation of CXCR7 inhibits the growth and lung metastasis of human hepatocellular carcinoma cells with highly metastatic potential. Exp Ther Med 2012;3:117-23.
[30] Gee MF, Tsuchida R, Eichler-Jonsson C, et al. Vascular endothelial growth factor acts in an autocrine manner in rhabdomyosarcoma cell lines and can be inhibited with all-trans-retinoic acid. Oncogene 2005;24:8025-37.
[31] de Nigris F, Rossiello R, Schiano C, et al. Deletion of Yin Yang 1 protein in osteosarcoma cells on cell invasion and CXCR4/angiogenesis and metastasis. Cancer Res 2008;68:1797-808.
[32] Pakos EE, Goussia AC, Tsekeris PG, et al. Expression of vascular endothelial growth factor and its receptor. KDR/Flk-1, in soft tissue sarcomas. Anticancer Res 2005;25:3591-6.
[33] Yudoh K, Kanamori M, Ohmori K, et al. Concentration of vascular endothelial growth factor in the tumour tissue as a prognostic factor of soft tissue sarcomas. Br J Cancer 2001;84:1610-5.
[34] West CC, Brown NJ, Mangham DC, et al. Microvessel density does not predict outcome in high grade soft tissue sarcoma. Eur J Surg Oncol 2005;31:1198-205.
[35] Schutyser E, Struyf S, Van Damme J. The CC chemokine CCL20 and its receptor CCR6. Cytokine Growth Factor Rev 2003;14:409-26.

A peptide antigen derived from EGFR T790M is immunogenic in non-small cell lung cancer

KAZUYA OFUJI[1,2], YOSHITAKA TADA[1,3], TOSHIAKI YOSHIKAWA[1], MANAMI SHIMOMURA[1], MAYUKO YOSHIMURA[1], KEIGO SAITO[1], YASUNARI NAKAMOTO[2] and TETSUYA NAKATSURA[1]

[1]Division of Cancer Immunotherapy, Exploratory Oncology Research and Clinical Trial Center, National Cancer Center, Kashiwa, Chiba; [2]Second Department of Internal Medicine, Faculty of Medical Sciences, University of Fukui, Fukui; [3]Research Institute for Biomedical Sciences, Tokyo University of Science, Noda, Chiba, Japan

Received August 29, 2014; Accepted October 9, 2014

DOI: 10.3892/ijo.2014.2787

Abstract. Lung cancer is the leading cause of cancer-related deaths worldwide. Epidermal growth factor receptor-tyrosine kinase inhibitors (EGFR-TKIs), such as gefitinib and erlotinib, have demonstrated marked clinical activity against non-small cell lung cancer (NSCLC) harboring activating epidermal growth factor receptor (EGFR) mutations. However, in most cases, patients develop acquired resistance to EGFR-TKI therapy. The threonine to methionine change at codon 790 of EGFR (EGFR T790M) mutation is the most common acquired resistance mutation, and is present in ~50% cases of TKI resistance. New treatment strategies for NSCLC patients harboring the EGFR T790M mutation are required. We evaluated the immunogenicity of an antigen derived from EGFR with the T790M mutation. Using BIMAS we selected several EGFR T790M-derived peptides bound to human leukocyte antigen (HLA)-A*02:01. T790M-A peptide (789-797) (IMQLMPFGC)-specific cytotoxic T lymphocytes (CTLs) were induced from peripheral blood mononuclear cells (PBMCs) of HLA-A2$^+$ healthy donors. An established T790M-A-specific CTL line showed reactivity against the NCSLC cell line, H1975-A2 (HLA-A2$^+$, T790M$^+$), but not H1975 (HLA-A2$^-$, T790M$^+$), and the corresponding wild-type peptide (ITQLMPFGC)-pulsed T2 cells using an interferon-γ (IFN-γ) enzyme-linked immuno spot (ELISPOT) assay. This CTL line also demonstrated peptide-specific cytotoxicity against H1975-A2 cells. This finding suggests that the EGFR T790M mutation-derived antigen could be a new target for cancer immunotherapy.

Correspondence to: Professor Tetsuya Nakatsura, Division of Cancer Immunotherapy, Exploratory Oncology Research and Clinical Trial Center, National Cancer Center, 6-5-1 Kashiwanoha, Kashiwa, Chiba 277-8577, Japan
E-mail: tnakatsu@east.ncc.go.jp

Abbreviations: aAPC, artificial antigen-presenting cell; ELISPOT, enzyme-linked immuno spot; HLA, human leukocyte antigen; IFN-γ, interferon-γ; MAPK, mitogen-activated protein kinase; PBMC, peripheral blood mononuclear cell; PI3K, phosphatidylinositol 3-kinase; PFS, progression-free survival; STAT, signal transducer and activator of transcription

Key words: acquired resistance, CTL epitope, EGFR T790M, immunotherapy, non-small cell lung cancer

Introduction

Lung cancer is the leading cause of cancer-related deaths worldwide (1). Non-small cell lung cancer (NSCLC) accounts for ~80% of all lung cancer cases. Despite recent development in treatment agents, the prognosis for lung cancer patients remains poor (2).

Overexpression of epidermal growth factor receptor (EGFR) is observed in various malignancies, including lung cancer (3). EGFR activation induces many intracellular signaling pathways, such as the mitogen-activated protein kinase (MAPK), phosphatidylinositol 3-kinase (PI3K), and signal transducer and activator of transcription (STAT) pathways, which cause tumor cell proliferation and survival (4). The EGFR pathway is an appropriate target for cancer therapy, and several agents that block this pathway have been developed. In particular, epidermal growth factor receptor-tyrosine kinase inhibitors (EGFR-TKIs), such as gefitinib and erlotinib, demonstrated marked clinical activity against NSCLC harboring an activating EGFR mutation (5-9). However, patients develop acquired resistance to EGFR-TKIs almost without exception (10). A secondary mutation, resulting in a threonine to methionine change at codon 790 of EGFR (EGFR T790M), is the major mechanism of EGFR-TKI resistance (10,11). Additionally, some reports suggest that the EGFR T790M mutation may not be rare and may exist in a small population of in tumor cells before TKI treatment (12-14). Moreover, a pre-existing T790M mutation was associated with shorter progression-free survival (PFS) in patients receiving TKI treatment (13,14). At this time, no standard treatment for EGFR mutant patients with acquired resistance has yet been established, and novel strategies for overcoming this resistance issue are required.

Immunotherapy for NSCLC patients is considered to be a potentially feasible option, because of its high specificity

and low toxicity against normal tissues; indeed, several tumor-associated antigen (TAA)-targeted phase 2/3 studies are ongoing (15). However, unfortunately, the results of a TAA-based vaccine therapy study were unsatisfactory (16). One concept for improving the effect of cancer vaccine therapy is to target mutated antigen-derived epitopes. It has been reported that various mutated epitopes were recognized by tumor-reactive T cells (17,18), suggesting that the mutated epitope was potentially immunogenic and thus might function as an immunotherapeutic target. There are few studies of immunotherapy targeting the EGFR T790M mutation. Here, we hypothesized that EGFR T790M-harboring cancer cells could be targeted by activated immune cells, and attempted to assess the immunogenicity of the EGFR T790M mutation-derived antigen *in vitro*. In the present study, we identified the human leukocyte antigen (HLA)-A2-restricted EGFR T790M mutation-derived epitope. Our results suggest that immunotherapy targeting the EGFR T790M mutation-derived antigen may be a novel treatment option for NSCLC patients with the T790M mutation. The combination of immunotherapy and EGFR-TKI therapy also may be a novel strategy for prevention of T790M-mediated resistance.

Materials and methods

Cell lines. The human NSCLC cell line H1975 was provided by Professor Seiji Yano (Kanazawa University, Ishikawa, Japan). H1975-A2 (H1975 transfected with HLA-A2) was provided by Dr Tetsuro Sasada (Kurume University, Fukuoka, Japan). Artificial APC-A2 (aAPC-A2) cells, which were generated by transduction of HLA-A*02:01, CD80, and CD83 molecules into K562 cells, were provided by Dr Naoto Hirano (Dana-Farber Cancer Institute, Boston, MA, USA). T2 cells (HLA-A*02:01, TAP$^-$) and human NSCLC cell line 11-18 were purchased from Riken (Saitama, Japan). These cell lines were cultured in RPMI-1640 (Sigma Chemical Co., St. Louis, MO, USA), supplemented with 10% FBS (Gibco-BRL, Carlsbad, CA, USA), 100 U/ml penicillin, and 100 μg/ml streptomycin in a humidified atmosphere containing 5% CO_2.

PBMC collection. Peripheral blood samples were collected from four HLA-A*02:01-positive healthy donors, after informed consent was obtained. Peripheral blood mononuclear cells (PBMCs) were isolated by density centrifugation using Ficoll-Hypaque (Pharmacia, Uppsala, Sweden) and frozen in liquid nitrogen until use.

Epitope prediction and synthesis. The epitope prediction software BIMAS (http://www-bimas.cit.nih.gov/molbio/hla_bind/) was used to predict peptides that could bind to HLA-A2. EGFR T790M mutation-derived peptides (purity >95%) were purchased from Scrum, Inc. (Tokyo, Japan). H-2 Kb-restricted ovalbumin (OVA) (257-264) (SIINFEKL) peptide (AnaSpec, Inc., Fremont, CA, USA) was used as a negative control in the peptide-binding assay. HLA-A2-restricted cytomegalovirus (CMV) (495-503) (NLVPMVATV) peptide was used as a positive control peptide, and an HLA-A2-restricted HIV-gag (77-85) (SLYNTYATL) peptide (American Peptide Company, Sunnyvale, CA, USA) as an irrelevant peptide in cytotoxic T lymphocyte (CTL) assays.

Peptide-binding assay. After incubation in culture medium at 26˚C overnight, T2 cells were washed with PBS and suspended in 1 ml Opti-MEM (Invitrogen Life Technologies, Carlsbad, CA, USA) with peptide (100 μg/ml), followed by incubation at 26˚C for 3 h and then at 37˚C for 2.5 h. After washing with PBS, HLA-A2 expression was measured using a BD FACSCanto II flow cytometer (BD Biosciences, San Jose, CA, USA) using a FITC-conjugated HLA-A2 (MBL Co., Ltd., Aichi, Japan)-specific monoclonal antibody. Mean fluorescence intensity (MFI) was analyzed using the FlowJo software (Tomy Digital Biology Co., Ltd., Tokyo, Japan). An OVA peptide was used as a negative control. A CMV peptide was used as a positive control peptide.

Generation of DCs. CD14$^+$ cells were isolated from PBMCs using human CD14 microbeads (Miltenyi Biotec GmbH, Bergisch Gladbach, Germany). Immature dendritic cells (DCs) were generated from CD14$^+$ cells using IL-4 (10 ng/ml; PeproTech, Inc., Rocky Hill, NJ, USA) and granulocyte-macrophage colony-stimulating factor (GM-CSF) (10 ng/ml; PeproTech, Inc.) in RPMI-1640 supplemented with 10% FBS. Maturation of DCs was induced by prostaglandin E2 (PGE2) (1 μg/ml; Sigma Chemical Co.) and tumor necrosis factor-α (TNF-α) (10 ng/ml; PeproTech, Inc.).

Induction of peptide-specific CTLs. CD8$^+$ cells were isolated using human CD8 microbeads (Miltenyi Biotec GmbH) from PBMCs. CD8$^+$ cells ($2x10^6$ cells/well) were stimulated with peptide-pulsed (10 μg/ml) 100-Gy-irradiated autologous mature DCs ($1x10^5$ cells/well) in RPMI-1640 containing 10% heat-inactivated human AB serum. After 1 week, these cells were stimulated twice weekly with peptide-pulsed (10 μg/ml) 200-Gy-irradiated aAPC-A2 cells ($1x10^5$ cells/well). Supplementation with 10 IU/ml IL-2 (Proleukin; Novartis, Basel, Switzerland) and 10 ng/ml IL-15 (PeproTech, Inc.) was performed at 3-4-day intervals between stimulations.

IFN-γ ELISPOT assay. Specific secretion of interferon-γ (IFN-γ) from human CTLs in response to stimulator cells was assayed using the IFN-γ enzyme-linked immuno spot (ELISPOT) kit (BD Biosciences), according to the manufacturer's instructions. Stimulator cells were pulsed with peptide for 2 h at room temperature and then washed three times. Responder cells were incubated with stimulator cells for 20 h. The resulting spots were counted using an ELIPHOTO counter (Minerva Tech, Tokyo, Japan).

CD107a assay and generation of a CTL line. CD8$^+$ cells isolated using human CD8 microbeads from cultured cells were incubated with peptide-pulsed T2 cells at a ratio of 2:1 for 3.5 h at 37˚C. CD107a-specific antibodies (BD Biosciences) were included in the mixture during the incubation period. CD8$^+$ CD107a$^+$ cells were sorted using a FACSAria II cell sorter (BD Biosciences). Sorted CTLs were stimulated, and the CTL line was established as described previously (19).

Cytotoxicity assay. Cytotoxic capacity was analyzed using the Terascan VPC system (Minerva Tech). The CTL line

Table I. Predicted EGFR T790M-derived peptides binding to HLA-A2.

Peptide name	Position	Length	Sequence	BIMAS score[a]
T790M-A	789-797	9	IMQLMPFGC	35.378
T790M-B	790-799	10	MQLMPFGCLL	51.77
T790M-C	788-797	10	LIMQLMPFGC	24.921
T790M-D	789-797[b]	9	IMQLMPFGV	495.288
T790M-E	789-797[c]	9	IMQLMPFGL	152.124
T790M-Awt	789-797	9	ITQLMPFGC	0.68

[a]Binding scores were estimated using the BIMAS software (http://www-bimas.cit.nih.gov/molbio/hla_bind/). [b,c]The cysteine (C) residue at position 797 was mutated to valine (V) and leucine (L), respectively. EGFR T790M, threonine to methionine change at codon 790 of EGFR.

was used as the effector cell type. Target cells were labeled in calcein-AM (Dojindo Molecular Technologies, Inc., Kumamoto, Japan) solution for 30 min at 37°C. The labeled cells were then co-cultured with the effector cells for 4-6 h. Fluorescence intensity was measured before and after the culture period, and specific cytotoxic activity was calculated using the following formula: % cytotoxicity = {1 - [(average fluorescence of the sample wells - average fluorescence of the maximal release control wells)/(average fluorescence of the minimal release control wells - average fluorescence of the maximal release control wells)]} x 100%.

Results

*Assessment of EGFR T790M-derived peptide binding to HLA-A*02:01 molecules.* As the candidates of HLA-A*02:01-restricted EGFR T790M-derived CTL epitopes, we selected five 9- or 10-mer peptides with high predicted HLA-A*02:01-binding scores, calculated using BIMAS software. Three of the five EGFR T790M-derived peptides had higher binding scores than the corresponding wild-type peptides. Some studies have reported that modified peptides with single amino acid substitutions exhibit improved affinity for HLA molecules and enhanced immunogenicity (20-22); thus, we also designed two modified peptides. These modified peptides with a substitution of Cys for Val (T790M-D) or Leu (T790M-E) at codon 797 showed higher binding scores (Table I).

Using the HLA-A2 TAP-deficient T2 cell line, the binding affinity of the five synthetic peptides to HLA-A2 was assessed. A peptide-binding assay showed that three EGFR T790M-derived peptides were able to bind to HLA-A*02:01 molecules. In particular, the binding capability of the T790M-A peptide to HLA-A*02:01 molecules was higher than that of the corresponding wild-type peptide. This result suggests that the single amino acid substitution at codon 790 improved the binding affinity for HLA-A*02:01 molecules. The binding affinities of two mutated peptides (T790M-D and -E) to HLA-A*02:01 were equivalent to that of the CMV peptide used as a positive control (Fig. 1).

Induction of EGFR T790M-derived peptide-specific CTLs from human PBMCs. To evaluate the immunogenic potential of the five predicted HLA-A*02:01-binding peptides derived from EGFR T790M, we attempted to induce peptide-specific

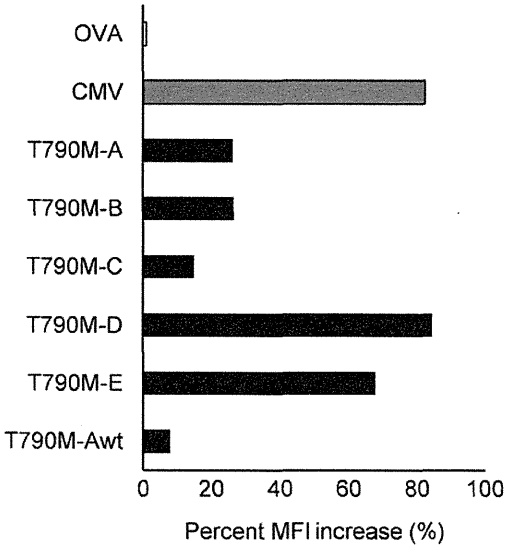

Figure 1. Binding of threonine to methionine change at codon 790 of EGFR (EGFR T790M)-derived peptides to human leukocyte antigen (HLA)-A2 molecule. A T2 binding assay was performed using a FACS system. An ovalbumin (OVA) peptide was used as a negative control. The bars show percent increases in mean fluorescence intensity (MFI). The average of two independent experiments is shown. (Percent MFI increase) = (MFI with the given peptide - MFI without peptide)/(MFI without peptide) x 100.

CTLs from human PBMCs obtained from four healthy donors. Several reports have shown the usefulness of artificial antigen-presenting cells (aAPCs) for the induction and expansion of peptide-specific CTLs from PBMCs (23,24). Thus, we attempted to induce such CTLs using aAPCs. $CD8^+$ cells were isolated from human PBMCs using human CD8 microbeads, and then stimulated with peptide-pulsed DCs for 1 week and subsequently, stimulated twice weekly with peptide-pulsed aAPC-A2 (Fig. 2A). As shown in Fig. 2B, ELISPOT assays revealed that T790M-A (789-797) (IMQLMPFGC)-specific CTLs were induced from PBMCs from all four donors. Also, induction of T790M-B (790-799) (MQLMPFGCLL)-specific CTLs were induced from PBMCs from two of the four healthy donors. However, stimulation with three other peptides, including modified peptides, did not induce peptide-specific CTLs. These results suggest that T790M-A (789-797) and T790M-B (790-799) have immunogenic potential and that

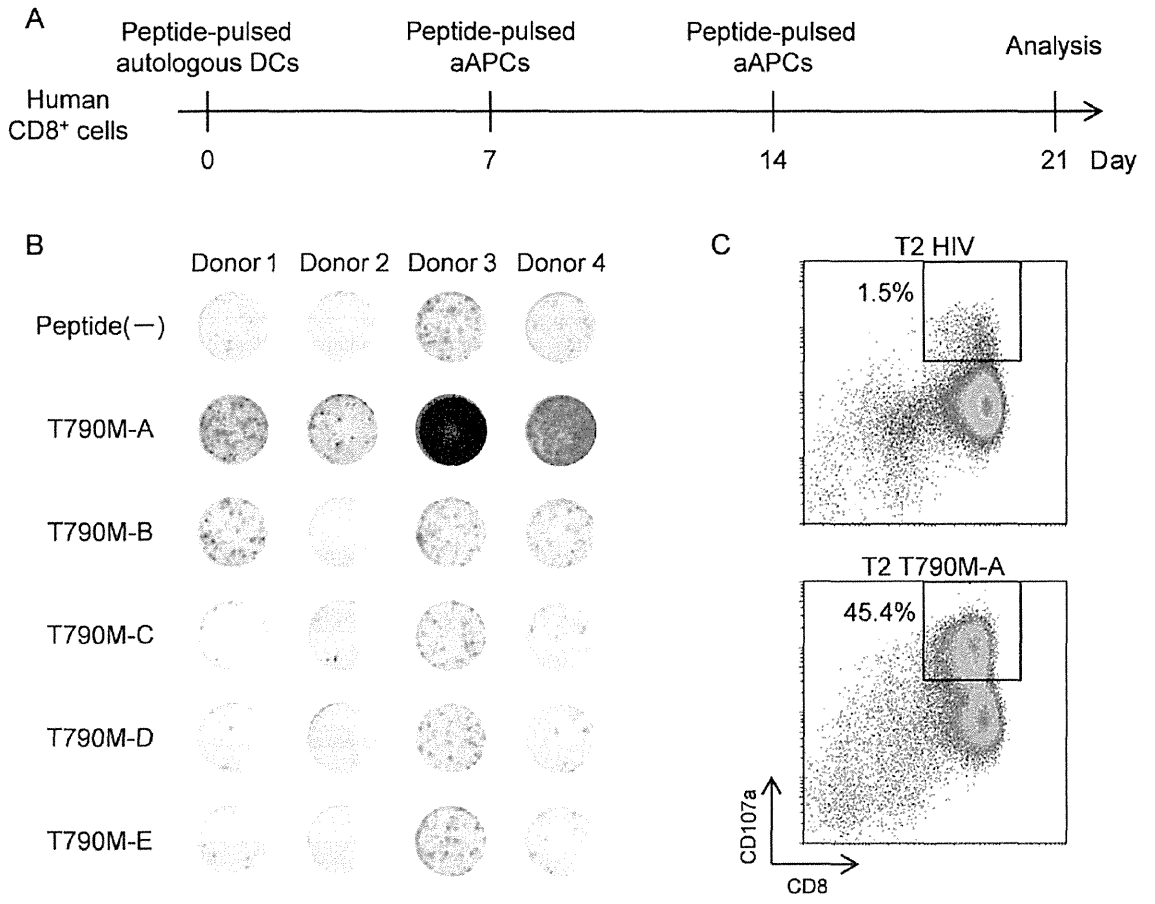

Figure 2. Induction of threonine to methionine change at codon 790 of EGFR (EGFR T790M)-derived peptide-specific cytotoxic T lymphocytes (CTLs) from peripheral blood mononuclear cells (PBMCs) of healthy donors. (A) Induction schedule of peptide-specific CTLs. $CD8^+$ cells ($2x10^6$ cells) isolated by anti-human CD8 microbeads from PBMCs were incubated with 10 μg/ml peptide-pulsed autologous dendritic cells (DCs) ($1x10^5$ cells) on day 0, followed by incubation with 10 μg/ml peptide-pulsed artificial antigen-presenting cell (aAPCs) ($1x10^5$ cells) on days 7 and 14. Peptide specificity was assessed by interferon-γ (IFN-γ) enzyme-linked immuno spot (ELISPOT) assay on day 21. (B) IFN-γ ELISPOT assay was carried out (effector, $1x10^5$ cells/well; target, $1x10^5$ cells/well) in duplicate at least three times independently; representative data are shown. (C) T790M-A-specific CTLs of healthy donor 3 were incubated with 10 μg/ml peptide-pulsed T2 cells (E:T = 2:1) for 3.5 h in the presence of an anti-human CD107a antibody. $CD8^+$ $CD107a^+$ cells were sorted using a FACSAria II cell sorter, which resulted in establishment of a T790M-A-specific CTL line.

CTLs specific for these peptides can be induced from human PBMCs. Given the effective induction of T790M-A (789-797) peptide-specific CTLs, we performed further analysis of the T790M-A peptide.

Generation of EGFR T790M-A-specific CTL line from human PBMCs. Next, we attempted to generate a purified T790M-A (789-797)-specific CTL line. Because the surface mobilization of CD107a is useful for identifying and isolating functional tumor-reactive T cells (25), we performed a CD107a assay to generate a purified T790M-A (789-797)-specific CTL line. Cultured cells stimulated by T790M-A peptide-pulsed DCs and aAPC-A2 *in vitro* were incubated with peptide-pulsed T2 cells at a ratio of 2:1 for 3.5 h at 37°C in the presence of an anti-CD107a antibody. More frequent $CD107a^+$ cells were observed when CTLs were co-cultured with T790M-A peptide-pulsed T2 cells compared to HIV-peptide-pulsed T2 cells, and $CD8^+$ $CD107a^+$ cells were sorted as a purified, peptide-specific CTL line using a FACSAria II cell sorter (Fig. 2C). A purified T790M-A-specific CTL line was established from healthy donor 3.

Cross-reactivity of the T790M-A-specific CTL line with other EGFR T790M-derived peptides. To assess its cross-reactivity with other EGFR T790M-derived peptides, the T790M-A-specific CTL line was cultured with T2 cells pulsed with each peptide, and IFN-γ production was measured by ELISPOT assay. The T790M-A-specific CTL line specifically recognized T2 cells pulsed with T790M-A (789-797) but not non-peptide-pulsed T2 cells. The T790M-A-specific CTL line did not recognize T2 cells pulsed with the T790M-A (789-797) wild-type (ITQLMPFGC) peptide. Also, T2 cells pulsed with T790M-B, -D, and -E were not recognized by the T790M-A-specific CTL line (Fig. 3A). However, the T790M-A-specific CTL line showed cross-reactivity with T2 cells pulsed with T790M-C.

Next, we evaluated the cytolytic activity of the T790M-A-specific CTL line against cognate peptide-pulsed T2 cells. The T790M-A-specific CTL line specifically lysed T790M-A peptide-pulsed T2 cells but not HIV-peptide-pulsed T2 cells (Fig. 3B). These results suggest that the T790M-A-specific CTL line showed cross-reactivity against some EGFR

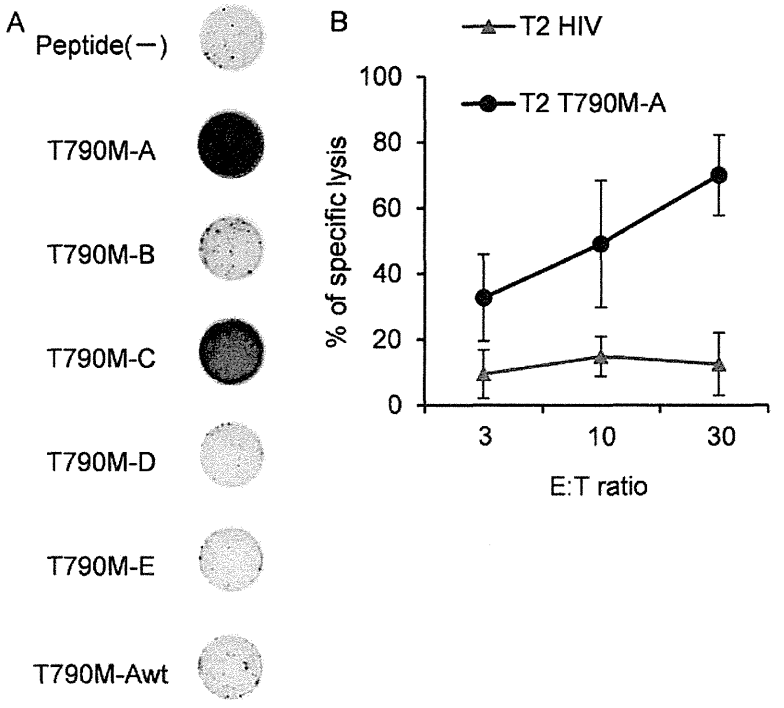

Figure 3. Cross-reactivity of the T790M-A-specific CTL line with threonine to methionine change at codon 790 of EGFR (EGFR T790M)-derived peptides. (A) Interferon-γ (IFN-γ) enzyme-linked immuno spot (ELISPOT) assay against T2 cells pulsed with each peptide. T2 cells pulsed with EGFR T790M-derived peptides (EGFR T790M-A, -B, -C, -D, -E, and Awt) were used as the target (effector $1x10^4$ cells/well, target $1x10^4$ cells/well). The assays were carried out in duplicate wells, and representative data are shown. (B) Cytotoxicity of the T790M-A-specific CTL line against T790M-A peptide-pulsed T2 cells. HIV-peptide-pulsed T2 cells were used as a negative control. Data are presented as means ± SD of three independent batches.

T790M-derived peptides, but not the corresponding wild-type EGFR-derived peptide. This cross-reactivity seems to be favorable for efficacy against EGFR T790M$^+$ cancer cells.

The T790M-A-specific CTL line recognizes and lyses HLA-A2$^+$ T790M$^+$ NCSLC cells. Next, we assessed the ability of the T790M-A-specific CTL line to recognize the HLA-A2$^+$ T790M$^+$ NCSLC cell line. This CTL line was incubated with 11-18 (T790M$^-$, HLA-A2$^+$), T790M-A-pulsed 11-18, H-1975 (T790M$^+$ HLA-A2$^-$), or H-1975-A2 (T790M$^+$ HLA-A2$^+$), and IFN-γ production was evaluated. We confirmed that the T790M-A-specific CTL line recognized peptide-pulsed 11-18 and H-1975-A2, but not 11-18 and H-1975, cells by IFN-γ ELISPOT assay (Fig. 4A). Similar data were obtained using CTLs from healthy donor 1 stimulated with T790M-A peptide-pulsed DC and aAPC-A2 *in vitro*, which were not purified by the CD107a assay (data not shown).

To evaluate the function of the T790M-A-specific CTL line against H1975-A2, a CD107a assay was performed. CD107a$^+$ cells were detected more frequently in culture with H-1975-A2 than with H-1975 cells (Fig. 4B).

Finally, we investigated the cytotoxic activity of the T790M-A-specific CTL line against H-1975-A2. Target cells were labeled with calcein-AM and co-cultured with the effector cells for 4-6 h. The T790M-A-specific CTL line showed cytotoxic activity against H1975-A2 cells, but not H1975 cells (Fig. 4C). These results suggest that the T790M-A-specific CTL line can recognize NSCLC cells harboring the EGFR T790M mutation in an HLA-A2-restricted manner.

Discussion

Mutated antigens associated with tumor cell progression and survival or drug resistance represent novel targets for cancer vaccine therapy. Warren *et al* evaluated computationally the antigenic potential of somatic mutations that occur in human cancers (26). They showed that several gene mutation-derived epitopes have immunogenic potential, at least computationally. Moreover, point mutations within the ABL kinase domain of the *BCR-ABL* gene are the most common causes of resistance to imatinib in chronic myeloid leukemia (CML) patients (27). Cai *et al* reported that the mutated *BCR-ABL* gene was associated with a TKI-resistance-generated CTL epitope in CML patients (28). These results suggest new immunotherapeutic approaches based on a TKI-resistant mutation-derived neoantigen. That is, mutations associated with acquired resistance to TKI therapy can be targeted by immune-based treatment strategies. This strategy may be an option to treat the gene mutation-mediated drug-resistant cancer cells. In the present study, we demonstrated the immunogenicity of antigens from mutated EGFR that are involved in TKI resistance in NCSLC.

TAAs can be classified into several categories, such as cancer-testis (CT) antigens, overexpressed antigens, differentiation antigens, and mutated antigens. Of these, only mutated antigens are unique, because they are not expressed in normal tissues. Previous reports have shown that peptide vaccine therapy can occasionally induce ineffective CTL responses, contrary to expectations (29-31). One possibility is

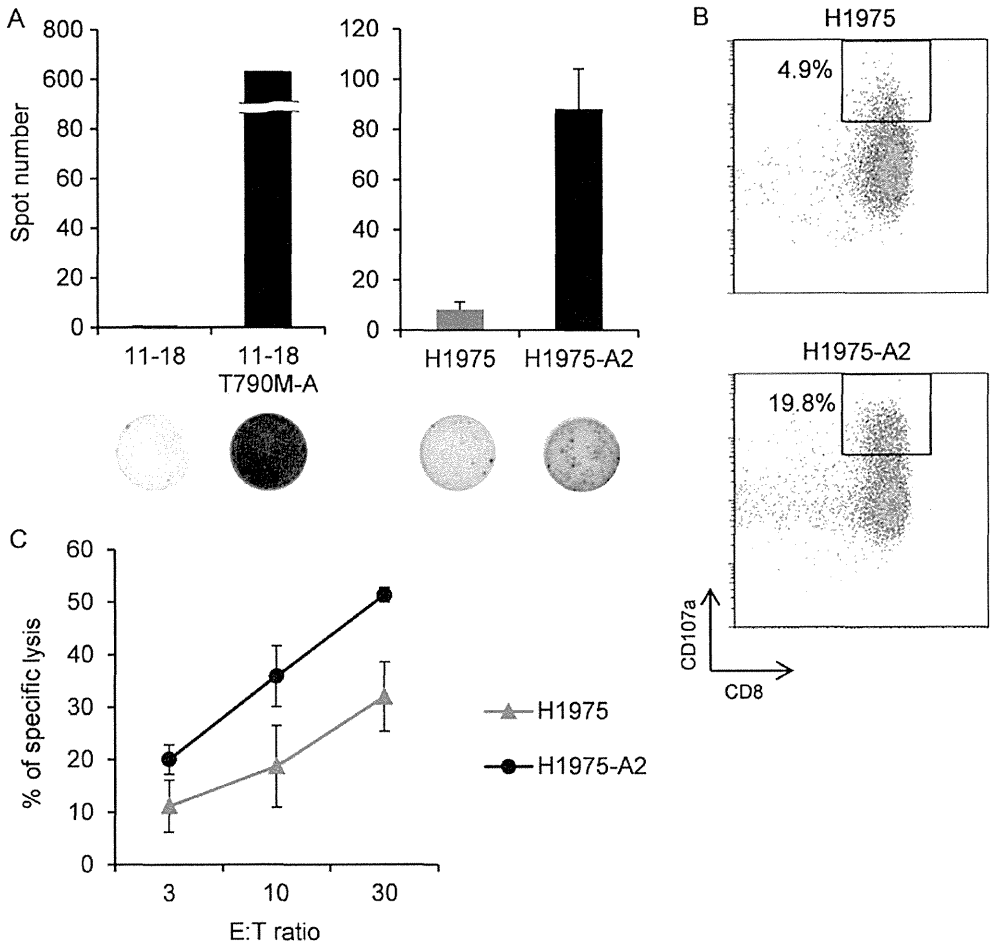

Figure 4. Reactivity of the T790M-A-specific CTL line against non-small-cell lung cancer (NSCLC) cells with or without the T790M mutation. (A) Interferon-γ (IFN-γ) enzyme-linked immuno spot (ELISPOT) assay results for the $T790M^+$ and $T790M^-$ NSCLC lines. Left: 11-18 and T790M-A peptide-pulsed (10 μg/ml) 11-18 cells were used as the targets (effector $1x10^5$ cells/well, target $1x10^5$ cells/well). Right: H-1975 and H1975-A2 cells were used as the targets (effector, $5x10^4$ cells/well; target, $5x10^4$ cells/well). The bars indicate the IFN-γ ELISPOT counts. (B) CD107a assay of the $T790M^+$ NSCLC line (E:T = 2:1). $CD8^+$ $CD107a^+$ cells were gated. (C) Cytotoxicity against the $T790M^+$ NSCLC cell line at the indicated effector/target ratios. Data are presented as means ± SD of three independent batches.

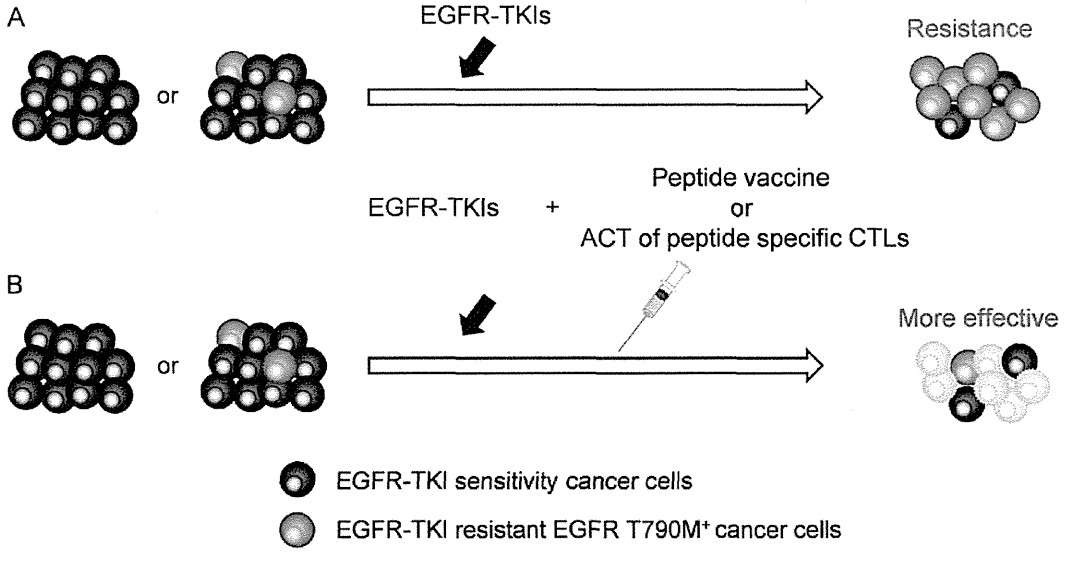

Figure 5. Combination therapy of epidermal growth factor receptor-tyrosine kinase inhibitor (EGFR-TKI) with T790M-targeted immunotherapy. (A) Generally, cancer cells develop acquired resistance to EGFR-TKI. (B) TKI-resistant cells harboring the T790M mutation were targeted by immunotherapy. This combination therapy may be effective against cancers with and without the threonine to methionine change at codon 790 of EGFR (EGFR T790M) mutation.

that the induced antigen-specific CTLs have a low affinity, and thus recognize only target cells pulsed with high concentrations of the peptide and not naturally presented epitopes on tumor cells. Several EGFR-derived CTL epitopes have been identified (32,33); however, the frequency of high-avidity EGFR-specific CTLs seems to be low in patients with EGFR-expressing cancers, because EGFR is a self-antigen that induces tolerance. The ability of low-avidity CTLs to recognize antigen-expressing tumor cells is considered to be weak. However, mutation-derived antigens are not self-antigens; thus, they would not be expected to induce immunotolerance, and so may have high immunogenicity. Indeed, in melanoma patients who experienced dramatic therapeutic effects after adoptive cell therapy with tumor-infiltrating lymphocytes (TILs), the mutated antigen-derived epitope was immunodominant and was recognized by tumor-reactive T cells (34,35).

In the present study, BIMAS was used to select EGFR T790M-derived candidate peptides that bind to HLA-A*02:01 according to computer algorithms, and T790M-A-specific CTLs could be induced from PBMCs of all four healthy donors by stimulation with peptide-pulsed DCs and aAPCs. Amino acid substitution of anchor residues (at position 2 and the C-terminus for HLA-A2) can alter the binding affinity (36-38). Leucine and methionine are the preferred anchor residues at position 2 of HLA-A2 (36,37). T790M-A (IMQLMPFGC) harbors a substitution of threonine to methionine at the anchor site, which confers immunogenicity. Also, valine and leucine are the preferred anchor residues at the C-terminus (36,37).

Then, we designed the modified peptides, T790M-D (IMQLMPFGV, substitution of cysteine to valine at the C-terminus) and T790M-E (IMQLMPFGL, substitution of cysteine to leucine at the C-terminus). These peptides bound to the HLA-A*02:01 molecule strongly (Fig. 1), but could not induce specific CTLs. T790M-D and -E are not self-antigens, being similar in this respect to T790M-A; this difference may be due in part to the difference in the frequency of peptide-specific CTL precursors. To confirm that the predicted candidate peptides are naturally presented peptides on tumor cells, peptide-specific CTL clones or lines induced by the peptides must recognize the tumor cells. A mass spectrometry (MS)-based method facilitates identification of peptide presentation by tumor cells (39). In this study, we confirmed the peptide-specific recognition of tumor cells by a peptide-specific CTL line, but not a CTL clone. However, CTL lines may contain distinct CTL clones that recognize irrelevant peptides, leading to apparent tumor reactivity (40). To avoid misleading tumor recognition and to evaluate the antigen-specific response of a CTL line, we used a peptide-specific CTL line established by CD107a sorting. An IFN-γ ELISPOT assay suggested that the specific CTL line recognized NSCLC cells harboring the EGFR T790M mutation in an HLA-A*02:01-restricted manner.

The T790M-A-specific CTL line did not show activity against the corresponding wild-type peptide. This suggests that EGFR T790M-targeted immunotherapy has no effect on NSCLC prior to EGFR-TKI treatment, with the exception of any pre-existing population of T790M-harboring cells, at least theoretically. Thus, consideration of combination therapy, EGFR-TKI and EGFR T790M-targeted immunotherapy, seems reasonable. Several studies have suggested that combination therapy could improve the efficacy of cancer immunotherapy. For instance, some chemotherapeutic agents can lead to upregulation of TAA expression or improvement of tumor cell resistance to specific CTLs (41). Use of an EGFR-TKI or anti-EGFR antibody augments the IFN-γ-induced expression of MHC classes I and II by A431 malignant human keratinocytes (42). Moreover, gefitinib improved the cytotoxic activity of natural killer cells against H1975 by modulating the interaction between NK cells and cancer cells, and by inhibiting STAT3 expression (43). These results indicate that the combination of EGFR-TKI and immunotherapy may have synergistic activity against NSCLC cells. The concept of combination therapy is shown in Fig. 5. Adding EGFR T790M-targeted immunotherapy to EGFR-TKI treatment could control the progression of cancer cells harboring T790M.

Yamada *et al* reported two HLA-A2-restricted EGFR T790M-derived CTL epitopes (790-799 MQLMPFGCLL and 788-798 LIMQLMPFGCL) (44). In addition to these epitopes, we identified the HLA-A*02:01-restricted CTL epitope T790M-A (789-797 IMQLMPFGC). We found that a T790M-A-specific CTL line established from human PBMCs had the ability to recognize and lyse the HLA-A*02:01$^+$ T790M$^+$ NCSLC cell line, and importantly, did not show cross-reactivity with the corresponding wild-type EGFR peptide. These results suggest that the EGFR T790M-A-specific CTL line recognizes single amino acid substitutions, leading to a low level of auto-immune reaction. The combination of an EGFR-TKI and T790M-targeted immunotherapy may be useful for treatment of NSCLC with the T790M mutation.

Acknowledgements

We thank Professor Seiji Yano for providing the NSCLC cell line H1975, Dr Tetsuro Sasada for providing the NSCLC cell line H1975-A2, and Professor Naoto Hirano for providing aAPC-A2. This study was supported in part by the National Cancer Center Research and Development Fund (25-A-7), as well as Research for the Promotion of Cancer Control Programmes, Research on Applying Health Technology, and Third Term Comprehensive Control Research for Cancer from the Ministry of Health, Labour, and Welfare, Tokyo, Japan.

References

1. Jemal A, Siegel R, Ward E, Murray T, Xu J and Thun MJ: Cancer statistics, 2007. CA Cancer J Clin 57: 43-66, 2007.
2. Youlden DR, Cramb SM and Baade PD: The international epidemiology of lung cancer: geographical distribution and secular trends. J Thorac Oncol 3: 819-831, 2008.
3. Normanno N, Maiello MR and De Luca A: Epidermal growth factor receptor tyrosine kinase inhibitors (EGFR-TKIs): simple drugs with a complex mechanism of action? J Cell Physiol 194: 13-19, 2003.
4. Hynes NE and Lane HA: ERBB receptors and cancer: the complexity of targeted inhibitors. Nat Rev Cancer 5: 341-354, 2005.
5. Mok TS, Wu YL, Thongprasert S, *et al*: Gefitinib or carboplatin-paclitaxel in pulmonary adenocarcinoma. N Engl J Med 361: 947-957, 2009.
6. Mitsudomi T, Morita S, Yatabe Y, *et al*: Gefitinib versus cisplatin plus docetaxel in patients with non-small-cell lung cancer harbouring mutations of the epidermal growth factor receptor (WJTOG3405): an open label, randomised phase 3 trial. Lancet Oncol 11: 121-128, 2010.

7. Maemondo M, Inoue A, Kobayashi K, *et al*: Gefitinib or chemotherapy for non-small-cell lung cancer with mutated EGFR. N Engl J Med 362: 2380-2388, 2010.
8. Zhou C, Wu YL, Chen G, *et al*: Erlotinib versus chemotherapy as first-line treatment for patients with advanced EGFR mutation-positive non-small-cell lung cancer (OPTIMAL, CTONG-0802): a multicentre, open-label, randomised, phase 3 study. Lancet Oncol 12: 735-742, 2011.
9. Rosell R, Carcereny E, Gervais R, *et al*: Erlotinib versus standard chemotherapy as first-line treatment for European patients with advanced EGFR mutation-positive non-small-cell lung cancer (EURTAC): a multicentre, open-label, randomised phase 3 trial. Lancet Oncol 13: 239-246, 2012.
10. Pao W, Miller VA, Politi KA, *et al*: Acquired resistance of lung adenocarcinomas to gefitinib or erlotinib is associated with a second mutation in the EGFR kinase domain. PLoS Med 2: e73, 2005.
11. Kobayashi S, Boggon TJ, Dayaram T, *et al*: EGFR mutation and resistance of non-small-cell lung cancer to gefitinib. N Engl J Med 352: 786-792, 2005.
12. Fujita Y, Suda K, Kimura H, *et al*: Highly sensitive detection of EGFR T790M mutation using colony hybridization predicts favorable prognosis of patients with lung cancer harboring activating EGFR mutation. J Thorac Oncol 7: 1640-1644, 2012.
13. Su KY, Chen HY, Li KC, *et al*: Pretreatment epidermal growth factor receptor (EGFR) T790M mutation predicts shorter EGFR tyrosine kinase inhibitor response duration in patients with non-small-cell lung cancer. J Clin Oncol 30: 433-440, 2012.
14. Rosell R, Molina MA, Costa C, *et al*: Pretreatment EGFR T790M mutation and BRCA1 mRNA expression in erlotinib-treated advanced non-small-cell lung cancer patients with EGFR mutations. Clin Cancer Res 17: 1160-1168, 2011.
15. Shepherd FA, Douillard JY and Blumenschein GR Jr: Immunotherapy for non-small cell lung cancer: novel approaches to improve patient outcome. J Thorac Oncol 6: 1763-1773, 2011.
16. Rosenberg SA, Yang JC and Restifo NP: Cancer immunotherapy: moving beyond current vaccines. Nat Med 10: 909-915, 2004.
17. Kawakami Y, Wang X, Shofuda T, *et al*: Isolation of a new melanoma antigen, MART-2, containing a mutated epitope recognized by autologous tumor-infiltrating T lymphocytes. J Immunol 166: 2871-2877, 2001.
18. Lennerz V, Fatho M, Gentilini C, *et al*: The response of autologous T cells to a human melanoma is dominated by mutated neoantigens. Proc Natl Acad Sci USA 102: 16013-16018, 2005.
19. Yoshikawa T, Nakatsugawa M, Suzuki S, *et al*: HLA-A2-restricted glypican-3 peptide-specific CTL clones induced by peptide vaccine show high avidity and antigen-specific killing activity against tumor cells. Cancer Sci 102: 918-925, 2011.
20. Valmori D, Fonteneau JF, Lizana CM, *et al*: Enhanced generation of specific tumor-reactive CTL in vitro by selected Melan-A/MART-1 immunodominant peptide analogues. J Immunol 160: 1750-1758, 1998.
21. Parkhurst MR, Salgaller ML, Southwood S, *et al*: Improved induction of melanoma-reactive CTL with peptides from the melanoma antigen gp100 modified at HLA-A*0201-binding residues. J Immunol 157: 2539-2548, 1996.
22. Fong L, Hou Y, Rivas A, *et al*: Altered peptide ligand vaccination with Flt3 ligand expanded dendritic cells for tumor immunotherapy. Proc Natl Acad Sci USA 98: 8809-8814, 2001.
23. Hirano N, Butler MO, Xia Z, *et al*: Engagement of CD83 ligand induces prolonged expansion of $CD8^+$ T cells and preferential enrichment for antigen specificity. Blood 107: 1528-1536, 2006.
24. Yoshimura M, Tada Y, Ofuzi K, Yamamoto M and Nakatsura T: Identification of a novel HLA-A*02:01-restricted cytotoxic T lymphocyte epitope derived from the EML4-ALK fusion gene. Oncol Rep 32: 33-39, 2014.
25. Rubio V, Stuge TB, Singh N *et al*: Ex vivo identification, isolation and analysis of tumor-cytolytic T cells. Nat Med 9: 1377-1382, 2003.
26. Warren RL and Holt RA: A census of predicted mutational epitopes suitable for immunologic cancer control. Hum Immunol 71: 245-254, 2010.
27. Soverini S, Hochhaus A, Nicolini FE, *et al*: BCR-ABL kinase domain mutation analysis in chronic myeloid leukemia patients treated with tyrosine kinase inhibitors: recommendations from an expert panel on behalf of European LeukemiaNet. Blood 118: 1208-1215, 2011.
28. Cai A, Keskin DB, DeLuca DS, *et al*: Mutated BCR-ABL generates immunogenic T-cell epitopes in CML patients. Clin Cancer Res 18: 5761-5772, 2012.
29. Yamshchikov GV, Barnd DL, Eastham S, *et al*: Evaluation of peptide vaccine immunogenicity in draining lymph nodes and peripheral blood of melanoma patients. Int J Cancer 92: 703-711, 2001.
30. Chen W, Yewdell JW, Levine RL and Bennink JR: Modification of cysteine residues in vitro and in vivo affects the immunogenicity and antigenicity of major histocompatibility complex class I-restricted viral determinants. J Exp Med 189: 1757-1764, 1999.
31. Meadows L, Wang W, den Haan JM, *et al*: The HLA-A*0201-restricted H-Y antigen contains a posttranslationally modified cysteine that significantly affects T cell recognition. Immunity 6: 273-281, 1997.
32. Shomura H, Shichijo S, Matsueda S, *et al*: Identification of epidermal growth factor receptor-derived peptides immunogenic for HLA-A2(+) cancer patients. Br J Cancer 90: 1563-1571, 2004.
33. Shomura H, Shichijo S, Komatsu N, *et al*: Identification of epidermal growth factor receptor-derived peptides recognised by both cellular and humoral immune responses in $HLA\text{-}A24^+$ non-small cell lung cancer patients. Eur J Cancer 40: 1776-1786, 2004.
34. Lu YC, Yao X, Li YF, *et al*: Mutated PPP1R3B is recognized by T cells used to treat a melanoma patient who experienced a durable complete tumor regression. J Immunol 190: 6034-6042, 2013.
35. Robbins PF, Lu YC, El-Gamil M, *et al*: Mining exomic sequencing data to identify mutated antigens recognized by adoptively transferred tumor-reactive T cells. Nat Med 19: 747-752, 2013.
36. Falk K, Rötzschke O, Stevanović S, Jung G and Rammensee HG: Allele-specific motifs revealed by sequencing of self-peptides eluted from MHC molecules. Nature 351: 290-296, 1991.
37. Sidney J, Southwood S, Mann DL, Fernandez-Vina MA, Newman MJ and Sette A: Majority of peptides binding HLA-A*0201 with high affinity crossreact with other A2-supertype molecules. Hum Immunol 62: 1200-1216, 2001.
38. Matsushita H, Vesely MD, Koboldt DC, *et al*: Cancer exome analysis reveals a T-cell-dependent mechanism of cancer immunoediting. Nature 482: 400-404, 2012.
39. Schirle M, Keilholz W, Weber B, *et al*: Identification of tumor-associated MHC class I ligands by a novel T cell-independent approach. Eur J Immunol 30: 2216-2225, 2000.
40. Parkhurst MR, Riley JP, Igarashi T, Li Y, Robbins PF and Rosenberg SA: Immunization of patients with the hTERT:540-548 peptide induces peptide-reactive T lymphocytes that do not recognize tumors endogenously expressing telomerase. Clin Cancer Res 10: 4688-4698, 2004.
41. Matar P, Alaniz L, Rozados V, *et al*: Immunotherapy for liver tumors: present status and future prospects. J Biomed Sci 16: 30, 2009.
42. Pollack BP, Sapkota B and Cartee TV: Epidermal growth factor receptor inhibition augments the expression of MHC class I and II genes. Clin Cancer Res 17: 4400-4413, 2011.
43. He S, Yin T, Li D, *et al*: Enhanced interaction between natural killer cells and lung cancer cells: involvement in gefitinib-mediated immunoregulation. J Transl Med 11: 186, 2013.
44. Yamada T, Azuma K, Muta E, *et al*: EGFR T790M mutation as a possible target for immunotherapy; identification of HLA-A*0201-restricted T cell epitopes derived from the EGFR T790M mutation. PLoS One 8: e78389, 2013.

Programmed death-1 blockade enhances the antitumor effects of peptide vaccine-induced peptide-specific cytotoxic T lymphocytes

YU SAWADA[1,2], TOSHIAKI YOSHIKAWA[1], MANAMI SHIMOMURA[1], TATSUAKI IWAMA[1], ITARU ENDO[2] and TETSUYA NAKATSURA[1]

[1]Division of Cancer Immunotherapy, Exploratory Oncology Research and Clinical Trial Center, National Cancer Center, Kashiwa, Chiba 277-8577; [2]Department of Gastroenterological Surgery, Yokohama City University Graduate School of Medicine, Kanazawa-ku, Yokohama 236-0004, Japan

Received September 7, 2014; Accepted October 17, 2014

DOI: 10.3892/ijo.2014.2737

Abstract. Novel treatment modalities are required urgently in patients with hepatocellular carcinoma (HCC). A vaccine that induces cytotoxic T lymphocytes (CTLs) is an ideal strategy for cancer, and glypican-3 (GPC3) is a potential option for HCC. Blocking the programmed death-1 (PD-1)/PD-L1 pathway is a rational strategy to overcome tumor escape and tolerance toward CTLs. In the present study, we investigated whether anti-PD-1 blocking antibodies (αPD-1 Ab) enhanced the number of vaccine-induced peptide-specific CTLs in peripheral blood mononuclear cells (PBMCs) following the administration of GPC3 peptide vaccine to both patients and in a mouse model. The inhibitory receptor PD-1 was highly expressed in *ex vivo* GPC3-specific CTLs isolated from the PBMCs of vaccinated HCC patients. *In vitro*, interferon-γ induced PD-L1 expression in liver cancer cell lines. In addition, PD-1 blockade increased the number of GPC3-specific CTLs, which degranulate against liver cancer cell lines. *In vivo* experiments using tumor-bearing mouse models showed that the combination therapy of peptide vaccine and αPD-1 Ab suppressed tumor growth synergistically. PD-1 blockade increased the number of peptide-specific tumor-infiltrating T cells (TILs) and decreased the expression of inhibitory receptors on TILs. This study demonstrated that PD-1/PD-L1 blockade augmented the antitumor effects of a peptide vaccine by increasing the immune response of vaccine-induced CTLs, and provided a foundation for the clinical development of a combination therapy using a GPC3 peptide vaccine and αPD-1 Ab.

Correspondence to: Dr Tetsuya Nakatsura, Division of Cancer Immunotherapy, Exploratory Oncology Research and Clinical Trial Center, National Cancer Center, 6-5-1 Kashiwanoha, Kashiwa 277-8577, Japan
E-mail: tnakatsu@east.ncc.go.jp

Abbreviations: HCC, hepatocellular carcinoma; CTL, cytotoxic T lymphocyte; GPC3, glypican-3; PD-1, programmed death-1; PBMC, peripheral blood mononuclear cell; HLA, human leukocyte antigen; IFN-γ, interferon-γ; MHC, major histocompatibility complex

Key words: programmed death-1, cytotoxic T lymphocyte, peptide vaccine, glypican-3, hepatocellular carcinoma

Introduction

Antigen-specific cancer immunotherapy using the induction of tumor-specific reactions without autoimmunity is a potentially attractive option for the treatment of cancer. However, immunotherapy for hepatocellular carcinoma (HCC) is still in the preclinical or early clinical trial phases (I and II) of development (1,2). Glypican-3 (GPC3), a carcinoembryonic antigen, is overexpressed in 72-81% of HCC cases, and is correlated with poor prognosis; therefore, it is an ideal target for HCC (3-7). Recently, a phase I clinical study of a GPC3-derived peptide vaccine reported its safety and efficacy for the treatment of advanced HCC (8). Although vaccine-induced GPC3-peptide-specific cytotoxic T lymphocytes (CTLs) are often tumor reactive *in vitro* (9) and correlate with overall survival, no complete response was observed when GPC3 peptide vaccination was used as monotherapy in patients with advanced HCC (8).

Programmed death-1 (PD-1) is expressed on activated T and B cells, and elicits inhibitory signals (10). Its ligand PD-L1 is member of the B7 family, and interacts with PD-1 (11). Several studies have shown that the PD-1/PD-L1 pathway plays a critical role in compromised tumor immunity (12,13). PD-1 antibody blockade exerts antitumor effects in clinical trials (14,15). High expression levels of PD-1 on T cells, both in tumor-infiltrating lymphocytes (TILs) and peripheral blood mononuclear cells (PBMCs), were correlated with poor prognosis in HCC patients after surgical resection (16). In addition, PD-L1 expression in HCC was correlated with tumor aggressiveness and postoperative recurrence (17).

In animal models, PD-1 blockade exerts synergistic effects with various tumor vaccines to enhance tumor antigen-specific T cell responses and suppress tumors *in vivo* (18-20). It was reported that melanoma vaccine-induced CTLs become exhausted, which could be reversed by blocking the inhibitory pathways (21). However, a study evaluating the combination

of a cancer vaccine and an anti-PD-1 blocking antibody (αPD-1 Ab) for HCC has not been conducted. Therefore, the aim of this study was to investigate whether αPD-1 Ab would enhance the antitumor effects of a peptide vaccine by analyzing CTLs isolated from the PBMCs of vaccinated patients, as well as from a mouse model.

Materials and methods

Patient samples. Three clinical trials were conducted using GPC3-derived peptide vaccines. A phase I trial (n=33) was performed in patients with advanced or metastatic HCC (8) (University Hospital Medical Information Network Clinical Trials Registry; UMIN-CTR no. 000001395). Subsequently, a phase II trial was performed using a GPC3-derived peptide vaccine as an adjuvant therapy in patients with HCC (UMIN-CTR: 000002614, on-going). Finally, a pilot study of liver biopsies taken before and after GPC3 peptide vaccination is being performed for advanced HCC (UMIN-CTR: 000005093, on-going). These trials were approved by the Ethics Committee of the National Cancer Center, Japan, and conformed to the ethical guidelines of the 1975 Declaration of Helsinki. All patients were enrolled after providing written informed consent. Patients were injected intradermally with HLA-A24-restricted $GPC3_{298-306}$ (EYILSLEEL) or HLA-A2-restricted $GPC3_{144-152}$ (FVGEFFTDV) peptide vaccines emulsified with incomplete Freund's adjuvant (IFA, Montanide ISA-51VG; SEPPIC).

Peripheral blood (30 ml) was obtained at the National Cancer Center Hospital East. PBMCs were isolated using standard Ficoll density gradient centrifugation from buffy coats. The remaining PBMCs were used after immunological monitoring in clinical trials. The immunological analyses were approved by the Ethics Committee of the National Cancer Center, Japan.

Cell lines. The human liver cancer cell lines SK-Hep-1 ($GPC3^-$, HLA-A*02:01/A*24:02), SK-Hep-1/GPC3 ($GPC3^+$, HLA-A*02:01/A*24:02), and HepG2 ($GPC3^+$, HLA-A*02:01/A*24:02) were available in our laboratory and were used as the target cells (6,9). SK-Hep-1/GPC3 is an established stable GPC3-expressing cell line that was transfected with the human GPC3 gene, whereas SK-Hep-1/vec is an established counterpart cell line that was transfected with an empty vector. The mouse lymphoma cell line RMA (OVA-, $H\text{-}2K^b$) was provided by Dr Yasuharu Nishimura (Kumamoto University, Japan). Cells were cultured at 37°C in RPMI-1640 or DMEM (Sigma-Aldrich) supplemented with 10% fetal bovine serum (FBS), 100 U/ml penicillin and 100 μg/ml streptomycin in a humidified atmosphere containing 5% CO_2.

Synthetic peptides and cytokines. The peptides used in this study were as follows: HLA-A*02:01-restricted $GPC3_{144-152}$ (FVGEFFTDV) peptide (American Peptide Co.), HLA-A*24:02-restricted $GPC3_{298-306}$ (EYILSLEEL) peptide (American Peptide Co.), HLA-A*02:01-restricted human immunodeficiency virus $(HIV)_{77-85}$ (SLYNTYATL) peptide (ProImmune), and $H\text{-}2K^b$-restricted ovalbumin $(OVA)_{257-264}$ (SIINFEKL) peptide (AnaSpec). The peptides were dissolved and diluted in 7% $NaHCO_3$ or dimethyl sulfoxide (DMSO). Where appropriate, liver cancer cell cultures were treated with 100 U/ml recombinant interferon (IFN)-γ (PeproTech).

Ex vivo Dextramer staining and flow cytometry. PBMCs were stained using HLA-A*02:01 Dextramer-RPE [$GPC3_{144-152}$ (FVGEFFTDV), HIV_{19-27} (TLNAWVKVV) or negative control; Immudex] and HLA-A*24:02 Dextramer-RPE [$GPC3_{298-306}$ (EYILSLEEL), $HIV_{583-591}$ (RYLKDQQLL); Immudex] for 15 min at room temperature, followed by anti-CD8-FITC (clone T8, Beckman Coulter), anti-PD-1-APC (clone EH12.2H7, BioLegend), or isotype control-APC (clone MOPC-21, BioLegend) for 20 min at 4°C. Flow cytometry was performed using a FACSCanto II (BD Biosciences).

Blocking antibody. GPC3 peptide-specific CTL clones were established from PBMCs as described previously (9). The CTL clones were cultured in AIM-V medium (Life Technologies) supplemented with 10% human AB serum in the presence of 10 μg/ml anti-PD-1 (clone J116, eBioscience) or 10 μg/ml control (clone MOPC-21, BioXcell) monoclonal antibodies for 2 days.

CD107a assay. GPC3 peptide-specific CTL clones were incubated with SK Hep-1/vec pulsed with $GPC3_{144-152}$ or HIV_{19-27} peptide and HepG2 at a 1:1 ratio for 3.5 h at 37°C. CTL clones were stained with anti-CD107a-APC (clone LAMP-1, BD Bioscience) during the incubation period, followed by anti-CD8-FITC (clone LT8, ProImmune) for 20 min at 4°C.

Mice. Female C57BL/6 mice (6-8 weeks old) were purchased from Japan Charles River Laboratories (Yokohama, Japan), and were maintained under specific pathogen-free conditions. The Animal Research Committee of the National Cancer Center, Japan, approved all studies. All animal procedures were performed according to the guidelines for the Animal Research Committee of the National Cancer Center, Japan. Ether was used for mouse euthanasia and anesthesia.

In vivo tumor growth inhibition assays. It was reported previously that intratumoral (i.t.) injection of $OVA_{257-264}$ peptide (SIINFEKL) effectively inhibited OVA-negative tumor growth and survival in a peptide vaccine model using C57BL/6 mice (22). RMA cells ($1x10^5$ cells/100 μl PBS) were implanted on the backs of C57BL/6 mouse on day 0. They were then injected with 50-μg peptide mixed with an equal volume of incomplete Freund's adjuvant (IFA, Montanide ISA-51VG; SEPPIC) on days 7 and 14. The total volume of injected vaccine solution was 100 μl in all experiments. For *in vivo* therapeutic experiments, anti-mouse PD-1 (clone 4H2) and control Ab (clone MOPC-21, BioXcell) were provided by Ono Pharmaceutical Co., Ltd. The anti-mouse PD-1 Ab (clone 4H2) used in the present study is a chimeric rat Ab containing the murine IgG1 Fc region (23). Anti-PD-1 or control Abs (200 μg/day) were injected intraperitoneally (i.p.) on days 7 and 14. Tumor volume was monitored twice per week, and was calculated using the following formula: tumor volume (mm^3) = a x b x b x 0.5, where a is the longest diameter, b is the shortest diameter, and 0.5 is a constant to calculate the volume of an ellipsoid. Mouse health, behavior and mortality were checked daily. All mice were maintained until they showed signs of morbidity or the

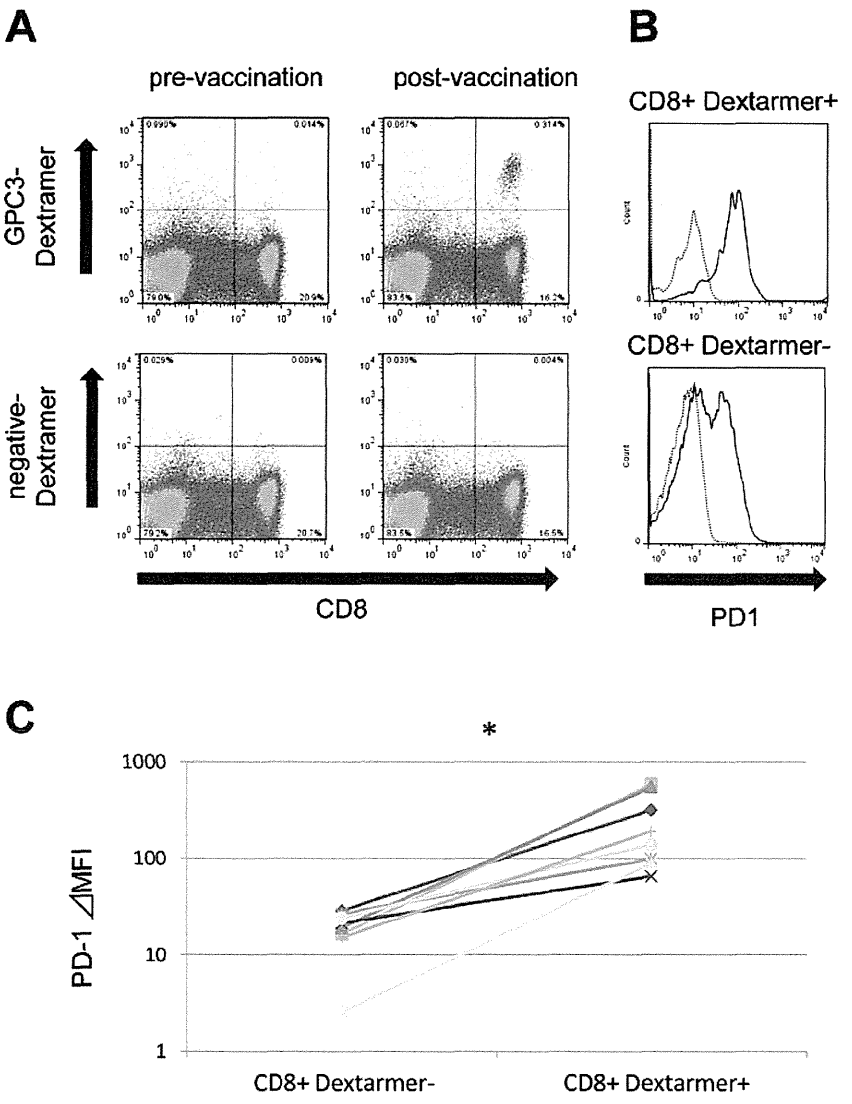

Figure 1. PD-1 expression on GPC3-specific CTLs after vaccination. (A) *Ex vivo* GPC3 Dextramer staining before and after vaccination in a representative case. The frequency of GPC3 peptide-specific CTLs is indicated as the percentage of the Dextramer-positive CTLs among PBMCs. (B) GPC3-specific CTLs were acquired by gating the CD8-positive/GPC3 Dextramer-positive population. The CD8-positive/GPC3 Dextramer-negative population was used as the control. (C) PD-1 expression on GPC3-specific CD8-positive/Dextramer-positive or -negative populations from eight patient specimens. ⊿, MFI, MFI using anti-PD-1 subtracted by that using isotype control. *P<0.05, n=8 using Wilcoxon's signed-rank test.

length or width of the tumors exceeded 30 mm, at which point they were sacrificed for reasons of animal welfare (22).

IFN-γ enzyme-linked immunospot (ELISPOT) analysis. The BD™ ELISPOT set (BD Biosciences) was used to assess the levels of IFN-γ, as described previously (24). Briefly, CD8-positive splenocytes ($5x10^5$) were added to the plate as effector cells. Then, either bone marrow-derived dendritic cells (BM-DCs; $1x10^5$) pulsed with OVA peptide (10 μg/ml; as target cells) or non-pulsed BM-DCs ($1x10^5$; as control cells) were added. The plate was then incubated for 37°C, for 20 h in the presence of 5% CO_2. Spots were counted automatically using the Eliphoto system (Minerva Tech).

Isolation of mouse tumors and flow cytometry. The mice were sacrificed and the dorsal tumors were dissected, cut into small pieces, and digested with collagenase (1 mg/ml) for 20 min at 37°C. After the intratumoral injection of $OVA_{257-264}$ peptide, tumor cells were isolated and stained with anti-mouse H-$2K^b$ bound to $OVA_{257-264}$ peptide (SIINFEKL)-PE (clone 25-D1.16, BioLegend) or isotype control-PE (MOPC-21, BioLegend). To analyze the local accumulation of antigen-specific CTLs in mice, isolated tumor cells including tumor-infiltrating lymphocytes were stained with H-$2K^b$ OVA Tetramer-PE [$OVA_{257-264}$ (SIINFEKL); MBL] for 30 min at room temperature. They were then incubated with anti-mouse CD8-FITC (clone KT15, MBL), anti-mouse PD-1-PE-Cy7 (clone 29F.1A12, BioLegend), anti-mouse CTLA-4-APC (clone UC10-4B, BioLegend), or anti-mouse LAG-3-PerCP-Cy5.5 (clone RTK2071, BioLegend) for 20 min at 4°C.

Quantitative real-time PCR. The tumors implanted into mice were dissected. Total RNA was isolated from homogenized tumors using RNeasy mini kit (Qiagen) according to

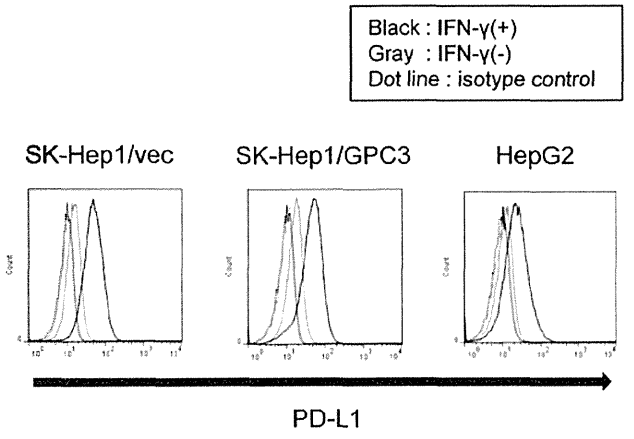

Figure 2. PD-L1 expression in liver cancer cell lines. Liver cancer cell lines were cultured with 100 U/ml IFN-γ for 24 h. PD-L1 expression was then analyzed using flow cytometry. Two independent experiments were performed, which yielded similar results.

the manufacturer's instructions. First-strand complementary deoxyribonucleic acid (cDNA) was synthesized using a PrimeScript® II first-strand cDNA Synthesis kit (Takara). Quantitative real-time PCR was then performed on an Applied Biosystems 7500 FAST Real-time PCR system using Power SYBR® Green (Applied Biosystems). We assessed the expression of the chemokines CXCL10, CXCL12, and CCL3, and compared them to *β-actin*. Data ware analyzed using delta-delta CT methods. Primer sequences of the chemokines were as described (25), and were purchased from Sigma Genosys.

Statistical analysis. All statistical analyses were performed using PASW Statistics software, version 18.0 (SPSS Inc.). Statistical significance was defined as a value of $P<0.05$ based on a two-tailed test.

Results

PD-1 expression ex vivo in GPC3 peptide-specific CTLs after vaccination in patients. To investigate whether vaccine-induced CTLs were affected by the PD-1/PD-L1 pathway, we measured the *ex vivo* expression of PD-1 on vaccine-induced GPC3-specific CTLs using flow cytometry with the GPC3-Dextramer. We used PBMCs obtained from eight patients during clinical trials of the GPC3 peptide vaccine. After vaccination, the frequency of GPC3-specific CTLs increased and could be detected *ex vivo*, as shown in the representative case 1 (Fig. 1A). GPC3-Dextramer-positive CD8 lymphocytes had a higher expression of PD-1 compared with GPC3-Dextramer-negative CD8 lymphocytes (Fig. 1B; representative case 1). In all eight patients with detectable GPC3-specific CTLs *ex vivo* after vaccination, PD-1 expression levels were significantly higher in GPC3-Dextramer-positive CD8 lymphocytes compared with GPC3-Dextramer-negative CD8 lymphocytes (Fig. 1C). Before vaccination, no GPC3-Dextramer-positive CD8 lymphocytes were detected *ex vivo*; therefore, PD-1 expression was not analyzed.

PD-1 blockade augments the GPC3-specific CTL clones that degranulate against liver cancer cell lines. SK-Hep1/vec, SK-Hep1/GPC3, and HepG2 liver cancer cell lines cultured with IFN-γ exhibited marked induction of PD-L1 on their surface (Fig. 2). This suggests that liver cancer cells are invaded by IFN-γ-producing CTLs via the PD-L1-mediated ligation of PD-1. Previously, several GPC3 peptide-specific CTL clones were established from PBMCs isolated from vaccinated patients. These clones exhibited cytotoxic activity

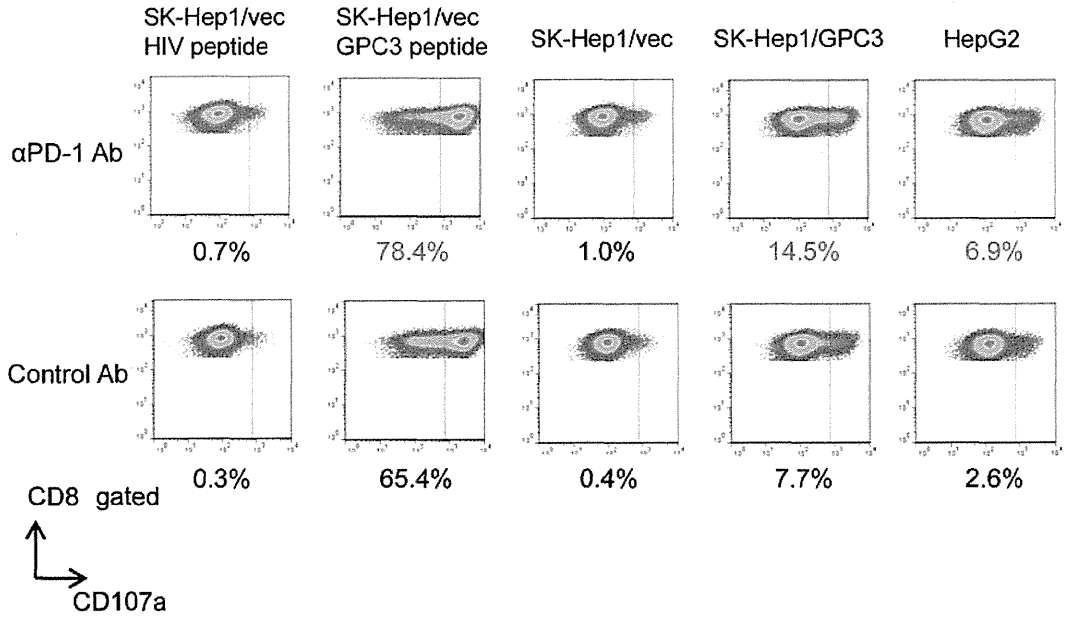

Figure 3. Blocking PD-1 increases GPC3-specific CTL clones that degranulate against liver cancer cell lines. The ratio of GPC3-specific CTL clones that externalized CD107a is shown below each column. The liver cancer cell lines used as the target cell are shown above each column. SK-Hep1/vec (GPC3$^-$) cells pulsed with peptide (1 μg/ml) were used as the target cells. The culture conditions are shown in rows. GPC3-specific CTL clones were acquired by gating the CD8-positive population. Two independent experiments were performed, which yielded similar results.